

Numerical analysis of heavy cob walls' hygrothermal behavior[☆]

Aguerata Kabore^a, Mathieu Bendouma^b, Claudiane Ouellet-Plamondon^{a,*}

^a Department of Construction Engineering, École de technologie supérieure, Université du Québec, 1100 Notre Dame Street West, Montreal, H3C 1K3, Canada

^b Département des sols et de génie agroalimentaire, Université Laval, 2325 Rue de l'université, Québec city, QC G1V 0A6, Canada

ARTICLE INFO

Keywords:

Hygrothermal simulations
Cob walls
Geosourced materials
Hygrothermal performance
Risk of mold

ABSTRACT

The development of building envelope systems with low carbon footprint materials and improved hygrothermal properties is still in progress. For geosourced materials, one of the main objectives is to achieve optimal hygrothermal efficiency. Cob, a material made of clay, plant fibres, and water, stands out for its low carbon footprint and ease of application on timber-framed building structures. The main goal of this study is to assess the hygrothermal performance of eight heavy cob wall systems in eight cities in African, European, and American climates. An extensive laboratory characterization is carried out to measure the hygrothermal properties of each material. The thermal conductivity obtained after the measurements is 0.75 W/m.K and 0.87 W/m.K for red and beige clay samples, respectively, 0.52 W/m.K for the cob with 3 % fibres, and 0.2 W/m.K for the cob with 6 % fibres samples, and the porosity rates are 21, 20, 37, and 45 for the clay and cob samples, respectively. The hygrothermal simulation showed that the interior temperature of the walls made of cob with 6 % fibres and a thickness of 25 cm remained stable, regardless of external climate variations. Applying beige clay plasters to the exterior and interior surfaces of cob walls or timber structures improved thermal performance in terms of heating or cooling energy demand but also increased the walls' moisture absorption. This increased moisture enhances the risk of mold growth within the wall structure. When used as infill materials in timber structures, the simulated composite systems generally exhibit good hygrothermal performance. However, in cold climate zones with high precipitation and heavily clouded skies, the walls may be exposed to risks of mold development. To prevent mold in these walls, install a rain screen or an air/vapor barrier membrane between the plaster and cob. This helps manage moisture and ensures proper wall drying.

1. Introduction

Regarding climate emergency, a global effort is aimed at reducing carbon emissions, especially in the energy and building sectors, for a greener economy by 2050 [1,2]. The study of local building materials and their use in modern construction is crucial for making buildings more energy-efficient and environmentally friendly. This approach promotes a sustainable architecture that considers energy efficiency and environmental protection [3–6]. A growing awareness translates into an increased commitment to design buildings with a low carbon footprint, stimulating numerous in-depth research on the passive cooling and heating features specific to earthen architecture [7,8]. Recent studies highlight the benefits of building with raw earth and bio-based materials, due to their abundant availability, affordable cost, non-toxicity, simple production processes, and recyclability [9–14]. These innovative approaches explore possibilities of industrialization, prefabrication,

mechanization, and digitization to enhance the reliability, performance, and efficiency of construction processes while maintaining reasonable costs [15–20].

Studies conducted on a hemp concrete building envelope at various thicknesses have revealed a good level of insulation with excellent thermal inertia [21–25], absorbing up to 90 % of daily variations in external temperature and relative humidity [22]. In the Moujalled and al. [22] study, using a wooden structure with hemp concrete led to air leakage. They recommend applying a continuous coating on the internal walls to solve this issue. The results of these studies have shown effective regulation of humidity, keeping it above 30 % during the heating period, and preventing the interior temperature from exceeding 27 °C in summer, even when the exterior temperature exceeds 35 °C [21,22]. Other studies have also emphasized the importance of the coating layer in humidity regulation and discussed the optimal thickness of this layer [26–31]. Hemp concrete, when combined with phase change materials,

[☆] This article is part of a special issue entitled: 'Decarbonising Built Env' published in Energy & Buildings.

* Corresponding author.

E-mail address: Claudiane.Ouellet-Plamondon@etsmtl.ca (C. Ouellet-Plamondon).

can effectively reduce fluctuations in interior temperature, provided it is properly positioned in the wall [32].

Earth materials have been studied, just like hemp concrete materials, and these studies have shown the benefits of using earth in eco-friendly and low-carbon footprint construction [33–38]. Research also explored the use of double walls made of hollow bricks enriched with bio-based earth, analyzed using EnergyPlus software, based on real building data. The results showed that this approach improved summer thermal comfort, reducing thermal dissatisfaction by 24.6 % compared to conventional constructions in hot climates [39]. Further simulations investigated the optimal thickness of these bio-based materials in various climates, revealing a notable reduction in heat loss and improved regulation of interior humidity and temperature [40,41]. These studies emphasize the importance of sustainable local materials, such as fibre-reinforced adobes, rammed earth, cob, and compressed earth blocks (CEB), for enhancing thermal comfort while reducing the environmental footprint of the construction sector. Earth materials mixed with plant fibres, in addition to having a low carbon footprint and being fully recyclable, offer an effective solution for reducing CO₂ emissions in construction by contributing to the elimination of plant fibres [42]. Earthen walls stabilize interior temperature and humidity through moisture absorption and desorption capacity. However, the use of waterproof coatings can limit their ability to regulate humidity, thereby increasing the risk of mold [33]. Despite these advantages, few studies have focused on cob and cob walls with wooden structures in hot, humid, and rainy areas. A thorough analysis is necessary to assess the influence of different external climates on building components, and to understand the heat and moisture transfer in these types of walls. The transfer of heat and moisture through building walls is a major cause of total building energy consumption and the appearance of mold on certain parts of these elements [34]. This phenomenon is influenced by the heat input from solar radiation, exterior air humidity, driving rain, and cloud cover (shading in the humid season). Studying the impact of humidity, cloud cover, and temperature on cob walls through numerical simulation is essential for understanding the long-term hygrothermal behaviour of these structures, whether in wattle and daub alone or with a wooden structure. This would help assess how temperature variations and humidity levels influence the performance of these walls.

Several studies on intrinsic energy, also known as embodied energy, which corresponds to the energy consumed for the extraction of raw materials, production, and construction of the building [43], have shown that the embodied energy of stabilized earth materials increases linearly with the cement content [44]. The total embodied energy of a stabilized earth wall containing 8 % cement is approximately 500 MJ/m³, which represents between 15 % and 25 % of that of fired clay brick walls. The embodied energy of compressed earth bricks and unstabilized rammed earth varies from 0 to 50 kWh/m³, with 3.94 MJ per brick, and overall embodied carbon of 0.39 kg CO₂eq per brick, or 47.5 kg CO₂eq/m³ [45]. Generally, the embodied carbon of earth and wood materials varies from 0.01 to 0.025 kg CO₂eq/kg of material [46,47]. The embodied carbon of reinforced concrete varies from 0.19 to 0.24 kg CO₂eq/kg of concrete, and for ordinary concrete, it varies from 0.10 to 0.16 kg CO₂eq/kg of concrete [47]. Regarding grey energy, some studies conducted on buildings made of cement blocks and clay block masonry have shown that buildings constructed with cement blocks emitted, during their construction, 452 kg CO₂eq/m², with a grey energy of 3198 MJ/m². In contrast, residential buildings constructed with clay block masonry emitted 235 kg CO₂eq/m² and had grey energy of only 1942 MJ/m² [48]. The grey energy of materials in an earth wall is about 20 times lower than that of a hollow and solid concrete block wall [49].

Cob walls, made from a mix of clay, water, and plant fibre, are recognized for their thermal mass capacity [50]. As with most building materials, cob is a porous material with various porosity levels. Moisture migration in these types of walls can lead to damage due to condensation [51]. Their susceptibility to moisture results in cracks and mold formation [52,53]. Moisture migration within the walls of a building can

affect not only the thermal and hydric characteristics of these walls but also energy consumption, interior air quality, and the building's lifespan [53,54]. Temperature has little influence on the thermal conductivity of materials reinforced with vegetable fibres [55]. Unlike temperature, relative humidity significantly impacts the thermal properties of cob material [56].

The numerical modeling examines various factors such as moisture absorption and drying, temperature, and humidity fluctuations, potential moisture-related damages over time, energy losses or gains for interior climate regulation, and moisture flows through the building envelope. Several simulation tools have been used to analyze thermal and moisture transfer in walls, including the Conduction Transfer Function (CTF) model [57,58], the effective moisture penetration depth (EMPD) model [59,60], the combined heat and moisture transfer (HAMT) model [55,58], COMSOL Multiphysics [61,62], and WUFI® [21,63,64]. The authors Yu et al. [57] used models based on the Conduction Transfer Function (CTF) and the Coupled Heat, Air, and Mass (HAM) algorithms to analyze the impact of coupled heat and moisture transfer on the indoor environment and energy consumption of buildings in several cities, including Harbin, Shenyang, Beijing, Shanghai, and Guangzhou. Their results show that this transfer has a significant influence on the annual energy consumption for heating and cooling, as well as on the thermal and humidity conditions inside buildings. Furthermore, Rahma et al. [58] validated the efficiency of the integrated HAMT model in EnergyPlus to predict the hygrothermal behavior of date palm concrete, a material recommended for sustainable construction in humid and semi-arid regions. In the work of Huibo et al. [59], the EMPD model was used to assess the hygroscopic performance of building materials, which influence indoor humidity and affect durability as well as air quality. They proposed indices for evaluating hygroscopic performance, validated through theoretical and experimental analyses. These results underline the importance of integrating environmental factors, such as air velocity, to obtain a more accurate assessment of building materials. Mariana et al. and Goffart et al. [55,60] also used these three models to check for the presence of minimum comfort parameters to better select the building envelope materials. They adopted a statistical approach to analyze the uncertainty and sensitivity of input data on the evaluation of the hygrothermal performance of building materials. Regarding COMSOL, Gerlich et al. [61] presented in their work the validation of the model using measured data from a segment of a real building. On the other hand, Chabani et al. [62], in their research, examine the quality of the experimental results and the numerical simulation, based on the mean squared errors between the two results. These mean squared errors serve as a measure of the accuracy of a model or an estimate compared to real values.

For the simulation with WUFI Pro, several authors have used this software to evaluate the hygrothermal response of single-layer and multi-layer walls based on meteorological data. Developed by the Fraunhofer Institute for Building Physics in Germany, WUFI Pro is specifically designed to analyze heat and moisture transfer in building envelopes. Talajji et al. [63] used the wall model of Doouzane et al. [65] to validate the WUFI Pro model to assess the hygrothermal performance of multi-layer straw walls, while Mesa [66] validated their numerical WUFI Pro model using experimental results from tests on a straw bale wall. In this article, the model was validated in the study by Kabore et al. [21] on the hygrothermal performance of hemp concrete walls, using the models of Dhakal et al. [67] and Lamalle [68], which also integrated experimental data to validate their model. These comparisons yielded consistent results, confirming the effectiveness of WUFI Pro as a reliable tool for evaluating the moisture dynamics within walls.

The evaluation of the hygrothermal performance of cob materials, through different wall system configurations, is a crucial step to ensure their effective and sustainable integration into modern construction as infill materials. This evaluation maximizes the benefits of cob while minimizing the risks associated with its use and promotes sustainable and responsible construction practices. Studies on biosourced and

geosourced materials, such as hemp concrete and adobe bricks, clearly show that these materials can play a significant role in the transition towards more eco-friendly and high-performance buildings. By integrating these materials into construction practices, it is possible to enhance not only the sustainability of buildings but also to contribute to the fight against climate change. To use cob in modern construction, which is also a geosourced material, it is essential to understand how this material reacts to climatic conditions. This study aims to anticipate future impacts on the performance of cob, allowing for proactive adjustments in construction techniques. Given that cob has not yet been widely studied in terms of hygrothermal performance, the results of this research will help better understand its behavior in response to external climatic conditions. This will also aid in identifying potential risks of material degradation, such as mold formation and deterioration due to excessive moisture.

The main objective of this study is to evaluate the long-term hygrothermal performance of two types of cob produced using traditional methods, for their application in the construction of modern contemporary buildings with a wooden frame structure. In this structural case, the wood is treated with Disodium Octaborate Tetrahydrate (DOT) to protect it against termites [69]. For this purpose, the hygrothermal performances of twelve wall systems were numerically studied using WUFI Pro 6.7 and COMSOL 6.1, two well-known simulation engines used to assess the hygrothermal performance of building envelopes. Two mathematical models were used in this study, one for WUFI Pro 6.7 and another for COMSOL 6.1. These software programs were employed to analyze the heat and moisture transfer through eleven cob walls, including four with 3 % fibres and seven with 6 % fibres. The evaluation of the evolution of temperature, humidity, energy, and moisture flow of the different walls was conducted considering factors such as orientation, cloudiness, and driving rain. As a result, the twelve wall systems, consisting of three single-layer walls and nine multi-layer walls, were assessed through WUFI Pro 6.7 simulations taking into account worst-case scenarios, wall orientation, driving rain, and cloudiness. For the simulation using COMSOL 6.1, only the three single-layer wall systems were analyzed. The aim of using these two models is to evaluate the impact of considering and not considering driving rain, cloudiness, capillary moisture, and the orientation of the walls on interior thermal comfort. Additionally, to assess the impact of considering the four elements on the risk of mold development, energy gains and losses, and moisture of the walls to regulate the interior environment. The particular challenge in modeling cob walls lies in their heterogeneity, with significant variations in density, porosity, and thermal conductivity, requiring detailed information on material properties. As a result, the production and data measurements for clay materials, clay plaster materials, and cob materials were carried out in the laboratory [50,70]. To achieve this, tests to determine the hygrothermal properties of the two types of cob used were conducted out in two different laboratories with samples of varying sizes. This was done to validate that there were no significant differences between the results obtained in the two laboratories and to ensure that sample size would not affect the thermal properties of the cob. Subsequently, the mechanical strength and volumetric shrinkage of the two types of cob were evaluated to ensure that these materials could be used in the construction of two-story or taller timber-framed buildings. The results are presented in our article [71]. Additionally, a thorough assessment of the influence of moisture on the hygrothermal properties of cob was also conducted prior to the numerical simulation, and these results are presented in the article by Kabore, A. and Ouellet-Plamondon, C. [56].

2. Materials and methods

2.1. Simulation methodology

In this study, WUFI Pro 6.7 software was used to analyze the heat and moisture flows necessary for interior climate regulation in a single layer

and multi-layer one-dimensional walls. Both factors can impact interior thermal comfort and wall material durability either negatively or positively. The software considers parameters such as cloudiness rate, driving rain, wall orientation for the worst possible case, and capillary rise in the wall's structure. It becomes necessary to evaluate the effects of these parameters on the evolution of the interior temperature, humidity, and the risk of mold growth in cob walls. On one hand, the model designed with WUFI Pro 6.7 software uses the coupled heat and mass transfer equation developed by Künzle [72,73]. On the other hand, the model designed with COMSOL 6.1 aims to evaluate the impact of the absence of cloudiness rates and driving rain on the evolution of temperature and humidity through cob walls. Simulations with COMSOL 6.1 were carried out on single-layer walls, as the simulation program is specifically designed for the analysis of single-layer walls. The numerical simulation does not take into account the protection of the walls by the roof, as the studied walls are susceptible to driving rain. The modeling is a hygrothermal modeling of the building's walls and not of the entire building.

2.2. Wall systems for simulation

The performance of eleven types of cob walls and one clay wall are studied through hygrothermal simulations using COMSOL 6.1 for the first three single-layer wall systems and with WUFI Pro 6.7 for all walls. An illustration of the different wall systems is presented in Tables 1 and 2. The hygrothermal properties of the wall materials are shown in Table 3, and the values of the effective thermal resistance (R) and the thermal transmission coefficients (U) of the walls obtained by WUFI Pro Software are presented in Tables 4 and 5.

2.3. Mathematical models

2.3.1. Energy and mass balance for WUFI pro and COMSOL multiphysics simulation

The building envelope made of cob, wood/cob, whether it is reinforced with few or many fibres, consists of porous materials. The envelope, that separates two environments (exterior and interior), is the site of heat and moisture transfers. The modes of transfers in these types of envelopes are thus the transfer of heat, liquid-phase water, and/or vapour-phase water [72]. Therefore, to realistically predict the hygrothermal behaviour of porous envelopes, it is necessary to consider the coupling of energy and mass transfers, as well as external climate events. The impact of energy and mass transfers in the envelopes is explained by the imbalance of heat flow, which results in a temperature variation across the envelope between the moment t and the moment $t + dt$, where dt is the time variation. Similarly, an imbalance of moisture flows (vapour in the liquid state) results in a variation (storage or release) of moisture across the envelope. An imbalance of vapour flows can lead to the adsorption or desorption of water (vapour condensation or water evaporation), involving latent heat (L_v), which is added to the thermal balance of the heat equation (Eqs. (2) and (8)). To analyze the hygrothermal performance of the cob formulations designed for the study project, a coupled modeling of heat and moisture transfer was implemented, and the influence of extreme temperature and humidity on the walls was evaluated. Fig. 1 shows the phenomena that occur in a wall and on the surfaces of a wall.

The numerical simulation with COMSOL 6.1 was carried out in a transient regime. The coupled mass and energy transfer equation is defined by Eqs. (1) and (2) [74].

$$\rho_s \frac{\partial w}{\partial HR} \frac{\partial HR}{\partial t} = -\nabla \cdot (- (D_v^{HR} + D_l^{HR}) \nabla HR - D_v^T \nabla T) \quad (1)$$

$$C_{mar} \frac{\partial T}{\partial t} = -\nabla \cdot (-\lambda \nabla T) - \rho_s \cdot c_{p_i} \cdot T \cdot \frac{d(Wm)}{dt} + \left(D_v^{HR} \frac{d(HR_x)}{dx} + D_v^T \frac{d(T_x)}{dx} \right) \cdot L_v \quad (2)$$

Table 1
Wall systems configuration, a) single-layer walls, b and c) Multilayer walls.

	Type I	Type II	Type III
a)			
Wall material	Red clay Type IV	Cob with 3 % fibre Type V	Cob with 6 % fibre
b)			
Exterior side	2.5 cm thick beige clay plaster 20 cm thick cob with 3 % fibre	2.5 cm thick beige clay plaster 20 cm thick cob with 6 % fibre	
Interior side	2.5 cm thick beige clay plaster Type VI	2.5 cm thick beige clay plaster Type VII	
c)			
Exterior side	2.5 cm thick spruce wood 20 cm thick cob with 3 % fibre	2.5 cm thick spruce wood 20 cm thick cob with 6 % fibre	
Interior side	2.5 cm thick spruce wood	2.5 cm thick spruce wood	

With ρ_s is the dry mass density of the material in kg/m^3 , C_{mat} is the thermal capacity of the material in J/kg.K , λ is the thermal conductivity in W/m.K , L_v is the constant latent heat of vaporization which is simplified to 2500 kJ/kg , C_{pl} is the thermal capacity of liquid water equal to 4186 J/kg K . The diffusion coefficients of water vapour D_v^{HR} , liquid water migration D_l^{HR} , water vapour thermodiffusion D_v^T , and saturation vapour pressure P_{vsat} , are expressed by Eqs. (3)–(6) [75].

$$D_v^{HR} = D_v \frac{M_v \cdot P_{\text{vsat}}(T)}{R \cdot T} \quad (3)$$

$$D_l^{HR} = \left(\frac{d w_m}{d H R} \right) \cdot \exp(p_1 - \frac{p_2}{W m}) \quad (4)$$

$$D_v^T = \frac{D_v \cdot M_v}{R \cdot T} \cdot H R \left(\frac{d(P_{\text{vsat}}(T))}{dT} - \frac{P_{\text{vsat}}(T)}{T} \right) \quad (5)$$

$$P_{\text{vsat}}(T) = P_{\text{atm}} \exp\left(\frac{13.7 - 5120}{T}\right) \quad (6)$$

With D_v is the water vapour diffusion coefficient, M_v is the molar mass of water in kg/mol , R is the ideal gas constant in J/mol K , T is the temperature in K , $W m$ is the water content of the material in kg/kg , P_{atm} is atmospheric pressure in Pa , $p_1 = -13.5$ and $p_2 = -0.015$ are adjustable parameters in Eq. (4) for plaster materials in the work of Bendouma [75]. These parameters are used by default in this article.

The software COMSOL 6.1 has already been used to solve the highly coupled hygrothermal transfer equations of porous materials [54,74–76]. The sorption curve of each material was adjusted using the GAB model to determine the model coefficients for numerical simulations on COMSOL 6.1 using Eq. (7). The GAB model (Guggenheim-

Anderson-de Boer) is widely used to describe water adsorption in porous materials, thanks to its ability to account for the interactions between water molecules and porous surfaces [77,78]. The model accurately represents adsorption isotherms, even in complex structures, thereby allowing the validation of experimental adsorption data [77]. Table 6 presents the GAB model coefficients for each material, and Fig. 2 shows the evolution of measured and evaluated, through GAB model, water content of the different materials.

$$w_m = \frac{(W_{GAB} \cdot C_{GAB} \cdot K_{GAB} \cdot H R)}{((1 - K_{GAB} \cdot H R)(1 - K_{GAB} \cdot H R + C_{GAB} \cdot K_{GAB} \cdot H R))} \quad (7)$$

Where w_m is moisture content absorbed by the material, in kg of water per kg of dry matter, W_{GAB} is the maximum amount of water the material can absorb, C_{GAB} is the the affinity of the material surface for water, K_{GAB} is the the isotherm shape correction coefficient, which adjusts the curvature of the isotherm and $H R$ is the relative humidity.

These conservation equations for mass and heat used for the simulation with the WUFI PRO 6.7 are presented by Eqs. (8) and (9) are developed in the articles by Künzel [72,73].

$$\frac{\partial w}{\partial H R} \cdot \frac{\partial H R}{\partial t} = \nabla \cdot (D_\varphi \nabla H R + \delta_p \nabla \cdot (H R P_{\text{sat}})) \quad (8)$$

$$\frac{\partial H}{\partial T} \cdot \frac{\partial T}{\partial t} = \nabla \cdot (\lambda \nabla T) + L_v \nabla \cdot (\delta_p \nabla \cdot (H R P_{\text{sat}})) \quad (9)$$

2.3.2. Boundary conditions

The energy and mass balance of the exterior surface at $x = 0$ is determined by Eqs. (10) and (11) using meteorological data such as the exterior temperature (T_{out}), the solar radiation (E_s) determined by Eq.

Table 2
Wall systems configuration, d and e) Multilayer walls.

	Type VIII	Type IX	Type XII
d)			
	1 1.5 20 1.5 1	1 1.5 20 1.5 1	
Exterior side	1 cm thick beige clay plaster 1.5 cm thick spruce wood 20 cm thick cob with 3 % fibre	1 cm thick beige clay plaster 1.5 cm thick spruce wood 20 cm thick cob with 6 % fibre	
Interior side	1.5 cm thick spruce wood 1 cm thick beige clay plaster Type X	1.5 cm thick spruce wood 1 cm thick beige clay plaster Type XI	
e)			
	2.5 0.1 20 2.5	2.5 0.1 20 2.5	2 1 0.1 20 2
Exterior side	2.5 cm beige clay 0.1 cm air/vapor barrier 3M™	2.5 cm spruce wood 0.1 cm air/vapor barrier 3M™	2 cm spruce wood 1 cm air gap
Interior side	20 cm cob with 6 % fibre 2.5 cm beige clay	20 cm cob with 6 % fibre 2.5 cm spruce wood	0.1 cm air/vapor barrier 3M™ 20 cm cob with 6 % fibre 2 cm spruce wood

Table 3
Hygrothermal properties of wall materials [50,70].

		Red clay	Beige clay	Cob with 3 % fibres	Cob with 6 % fibres	Spruce wood
Density	(kg/m ³)	2016	1956	1654	1412	400
Thermal conductivity	(W/m.K)	0.75	0.87	0.52	0.20	0.087
Specific heat	(J/kg.K)	901	930	917	944	1880
Water vapour resistance (dry)	(-)	14.52	20	15.11	14.71	552
Water vapour resistance (wet)	(-)	3.57	4.95	4.64	5.32	-
Porosity	(-)	20.63	20.12	37.14	45.43	0.9
Water content at 80 % RH	(%)	3.22	2.32	3.57	3.63	55.8
Free water saturation	(%)	159.91	141.73	132.37	119.32	845

Table 4
Thermal resistance (R) and thermal transmittance (U) value for each wall.

Walls	Type I	Type II	Type III	Type IV	Type V	Type VI	Type VII	Type VIII	Type IX
R-Value (m ² .K)/W	0.26	0.38	0.98	0.44	1.04	0.96	1.56	0.75	1.35
U-Value W/(m ² .K)	2.23	1.76	0.86	1.60	0.82	0.87	0.57	1.07	0.65

(15), the exterior humidity (HR_{out}), and the exterior atmospheric pressure. The energy and mass balance of the interior surface at $x = L$ is derived from the interior temperature, interior humidity, and interior atmospheric pressure and expressed by Eqs. (12) and (13).

$$\varphi_{T(x=0)} = hcv_{out} \cdot (T_{out} - T_{x=0}) + \varepsilon \cdot \sigma \cdot F \cdot (T_{sky}^4 - T_{x=0}^4) + \alpha \cdot E_s + L_v \varphi_{M(x=0)} \tag{10}$$

$$\varphi_{M(x=0)} = \dot{h}_{M_{out}} \frac{M_V}{R} \left(\frac{HR_{out} P_{vsa}(T_{out})}{T_{out}} - \frac{HR_{x=0} P_{vsa}(T)}{T} \right) \tag{11}$$

$$\varphi_{T(x=L)} = hcv_{in} \cdot (T_{in} - T_{x=L}) + \varepsilon \cdot \sigma \cdot F \cdot (T_{in}^4 - T_{x=L}^4) + L_v \varphi_{M(x=L)} \tag{12}$$

Table 5
Thermal resistance (R) and thermal transmittance (U) value for each wall with air/vapor barrier.

Walls	Type X	Type XI	Type XII
R-Value (m ² .K)/W	1.04	1.55	1.58
U-Value W/(m ² .K)	0.82	0.58	0.57

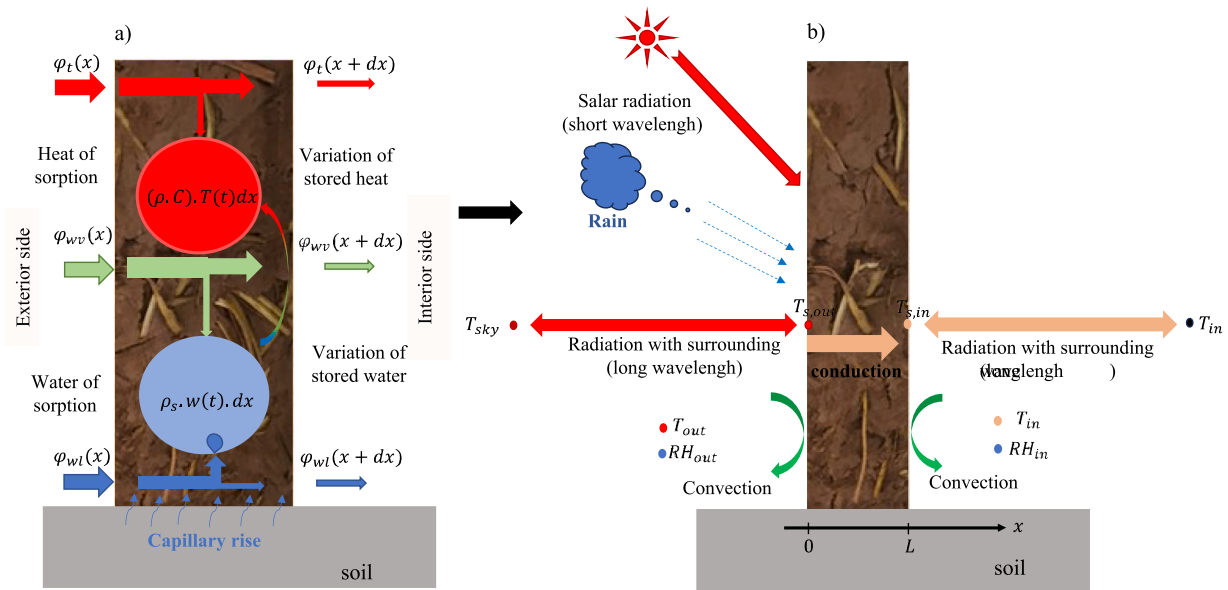


Fig. 1. Interactions between the external and internal environment and a hygroscopic wall, a) heat and moisture storage in the wall, b) heat or moisture exchange between external and internal surfaces.

Table 6
GAB coefficients for the COMSOL 6.1 simulation.

Type of material	W_{gab}	C_{gab}	K_{gab}
Clay	0.011	50	0.83
Cob3%f	0.012	35	0.82
Cob6% f	0.013	16	0.081

$$\varphi_{M(x=L)} = h_{Mins} \frac{M_V}{R} \left(\frac{HR_{x=L} P_{vsat}(T_{x=L})}{T_{x=L}} - \frac{HR_{ins} P_{vsat}(T_{ins})}{T_{ins}} \right) \quad (13)$$

Where hcv_{out} and hcv_{in} are the coefficients of external and internal convection respectively determined by Eqs. (16) and (17), relationships suggested by ASHRAE, and the fictive sky temperature (T_{sky}) determined by Eq. (18) [79]. The mass exchange coefficient h_M is derived from the Lewis relation given by Eq. (14) [75]. σ is the Stefan-Boltzmann constant, F is the shape factor, α the short-wave absorptivity of the material, ϵ is the long-wave emissivity, and P_{vsat} is the saturation vapour pressure.

$$h_M = \frac{h_{cv}}{\rho C_p L e^{2/3}} \quad (14)$$

$$E_s = \frac{1 + \cos(\Sigma)}{2} E_{diffH} + \frac{\cos(\theta)}{\sin(\beta)} E_{dirH} + \omega \frac{E_{meas}(1 - \cos(\Sigma))}{2} \quad (15)$$

$$hcv_{out} = 1,53.V_w + 1,43 \quad (14)$$

$$hcv_{in} = 1,5.(T_{x=L} - T_{in})^{1/3} \quad (17)$$

$$T_{sky} = T_{out} - 9 \quad (18)$$

Where E_{meas} is the sum of horizontal direct irradiation (E_{dirH}) and horizontal diffuse irradiation (E_{diffH}) (meteorological data), $\Sigma = \pi/2$ for vertical walls, θ is the angle of incidence (meteorological data), $\beta = 90^\circ$ for vertical walls, and ω is the ground reflectivity equal to 0.2 in this study [80], and V_w is the wind speed (meteorological data).

2.3.3. Simulation assumptions

This study focuses on the numerical modeling of the hygrothermal behaviour of nine wall systems. The COMSOL 6.1 model, developed for the simulation of single-layer walls, was used for the numerical simulation of walls of Type I, Type II, and Type III. The assumptions made to carry out the simulation are presented as follows:

1. The gaseous phase consisting of water vapor and air obeys the ideal gas law. The different solid-liquid-vapor phases are in thermodynamic equilibrium, and the fluids absorbed in the porous medium are incompressible and continuous.
2. Solar flows, ambient temperature, and humidity are time-dependent. Climate data from January 01, 2022, to January 01, 2023 were used.
3. The interior temperature was set to $24 \pm 2^\circ\text{C}$ for cities with hot and arid climates, and to $21.9 \pm 2^\circ\text{C}$ for cities with cold and humid

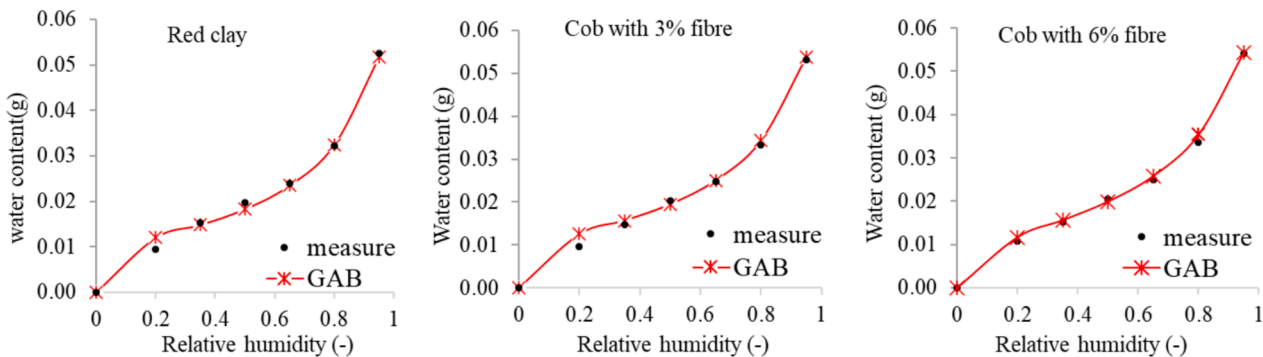


Fig. 2. Water adsorption isotherms for clay and cob materials.

climates, with interior humidity at $50 \pm 10 \%$, in accordance with ANSI/ASHRAE Standard 55 [81].

4. The initial relative temperature and humidity of the walls are uniform and set at $20 \text{ }^\circ\text{C}$ and 50% .
5. The short-wave absorptivity (α) of the materials is set at 0.7 for cob and clay walls, in accordance with the literature [82,83].
6. For long-wave radiative exchanges, the shape factors are expressed by $F = \frac{(1+\cos(\beta))}{2}$ with $\beta = \frac{\pi}{2}$ for vertical walls [84] (our case study), and the interior radiation temperature equal the interior temperature.
7. The long-wave emissivity (ϵ) of the materials is set at 0.9, a value obtained in WUFI Pro 6.7.

For the WUFI Pro 6.7 simulations, the nine wall systems were simulated with the following assumptions:

1. The assumptions 1, 2, 3, 4, 5, 6 and 7 applied for the COMSOL 6.1 simulation were applied.
2. The short-wave absorptivity (α) takes into account the material of the outer surface of multilayer walls.
3. The orientation of the walls is chosen for the worst case of driving rain. The amount of rain hitting the wall is calculated according to ASHRAE Standard 160 based on wind speed and direction, with the wall's exposure factor to rain (FE) equal to 1.4 and the rain deposition factor on the wall (FD) equal to 0.5.
4. For the simulation period presented in point 1, climate data from 3 years were used for the WUFI Pro 6.7 simulations, from January 1, 2020, to January 1, 2023, and the results of January 1, 2022, to January 1, 2023, were analyzed.
5. The average annual cloudiness index applied to the exterior environment for each city was taken into account, and this data is presented in the section 2.3.4 in Table 7.

In this study, the validation of the WUFI Pro model was conducted using data from Dhakal et al [67] and Lamalle [68]. The details and results are presented in the referenced works [21]. Dhakal et al. [67] analyzed the impact of mix proportions on the properties of hemp concrete and the hygrothermal performance of two hemp concrete walls, each 33.5 cm thick, designed for construction in Ontario, Canada. Meanwhile, Lamalle [68] examined five wall configurations to evaluate the hygrothermal performance of wood concrete for the city of Liège. Among these configurations, a 26 cm thick wood concrete wall was used to validate our model. The results of the numerical simulations performed with our model align perfectly with the findings of both authors, thus confirming the reliability and accuracy of our approach.

For the COMSOL model, two studies using the same model for the numerical simulation of insulated walls, validated by experimental data, allowed the model to be considered reliable. The results of the simulations were compared to the experimental results, which aligned with these experimental findings [75,85]. The COMSOL model was used in this study to evaluate the thermal performance of the rammed earth material in wall form, without considering cloud cover and heavy rain, and was used for the simulation only with the three single-layer walls

presented in section 2.2. For a simulation with multilayer walls, although the results presented in the authors' works [75,85] pertain to multilayer walls, validation of the model with experimental data from cob walls would be necessary.

2.3.4. Climate data

The climatic data of the cities of Djibouti, Johannesburg, Cairo, Abidjan, Montreal, Paris, Rennes and Reno were used to evaluate the hygrothermal performance of different cob walls. In total, the climatic data of 8 cities consisting of cities with hot and arid climates, cold and humid climates, and temperate climates were used. The purpose of using variable climatic data is to analyze the capacity of cob walls to regulate interior temperature in climates with high temperatures and the damage that can be caused by exterior climates with very high humidity to cob walls. The external climatic parameters were obtained from the Weather API for the years 2012 to 2023 [86]. Figures S1–S8 presented in the supplementary document illustrate the meteorological data parameters from January 1, 2022, to January 1, 2023, of the cities. Table 7 summarizes the maximum and minimum values of some climatic parameters of each city for the year 2022–2023. To facilitate the analysis of the results, the cities were grouped into two zones. The hot and temperate climate zone represents the cities of Djibouti, Johannesburg, Cairo, and Abidjan, while the cold climate zone represents the cities of Montreal, Paris, Rennes, and Reno (Table 7).

3. Results

To identify the best construction approach for each of the eight chosen locations, we evaluated eleven different cob wall configurations as outlined in Table 1. These walls were oriented to face the worst-case scenario for each locality, where precipitation is most intense. The results obtained from WUFI Pro 6.7 and COMSOL 6.1 data include temperatures, relative humidity, as well as heat and moisture flows, depending on the time and thickness of the material studied. The analysis of the walls' hygrothermal behaviour is based on hygrothermal criteria, with a critical humidity threshold set at 80% at every point in the wall. The goal of these simulations is to identify risks of condensation, mold growth, and thermal comfort issues for each climatic zone, and to offer recommendations for a better-adapted design.

3.1. Evaluation of temperature and humidity of the wall Type I to Type III

The evolution of temperature, independent of cloudiness and precipitation rates, was analyzed using COMSOL 6.1, while the impact of these two factors was studied with WUFI Pro 6.7. The average annual cloudiness rate for each city was calculated by WUFI Pro 6.7 using hourly climate data from each city, and this coefficient was associated with precipitation. Examining Fig. 3, the effect of cloudiness and heavy rain on the evolution of the interior temperature of clay and cob walls with a thickness of 25 cm is visible. Moreover, the temperature of the interior surface of the clay wall (Wall type I), not exposed to rain and cloudiness, reacts more to external climate variations, followed by the

Table 7
Summary of the hourly meteorological data for the year 2022–2023: Weather API [86].

Climate zone	City	Temperature °C		Relative Humidity %		Global radiation W/m ² max	Nebulosity – Average	Amount of rainwater l/(m ² .h)	
		min	max	min	max			min	max
Hot-temperate-climate zone	Djibouti	23	40	30	90	1050	0.31	0	2
	Johannesburg	0	42	10	80	1100	0.11	0	0.1
	Cairo	5	43	5	95	1050	0.18	0	2.5
	Abidjan	24	30	50	90	950	0.71	0	25
Cold-temperate-climate zone	Montreal	–26	36	20	100	950	0.64	0	3
	Paris	–6	40	20	100	950	0.4	0	8
	Rennes	–7	38	17	100	900	0.39	0	6
	Reno	–20	36	7	100	950	0.45	0	12.5

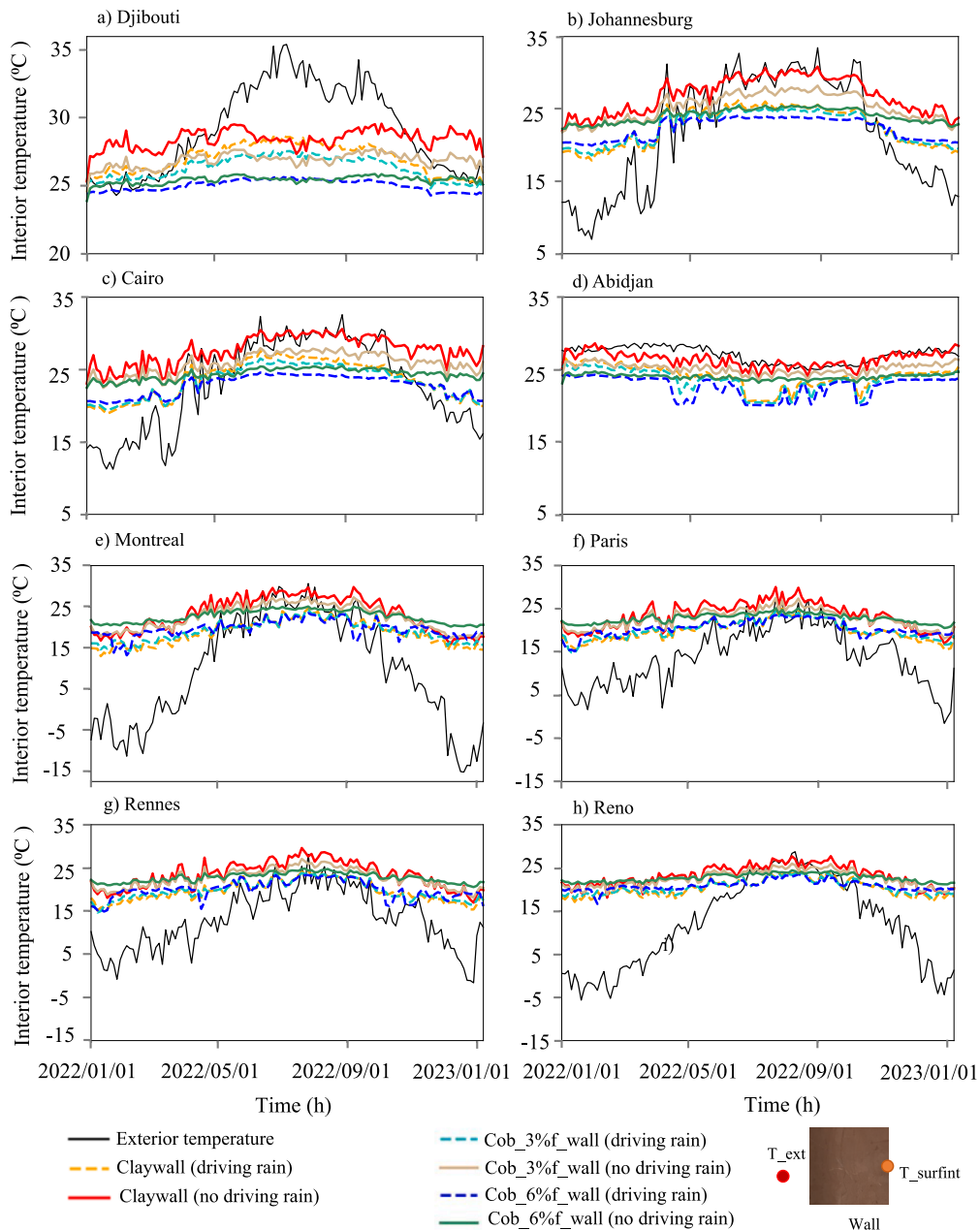


Fig. 3. Influence of driving rain on the daily interior surface temperature of uncoated clay and cob walls for the eight cities studied.

cob wall with 3 % fibres (Wall type II) and the one with 6 % fibres (Wall type III), respectively. The exposure of the three walls to heavy rain and cloudiness influences the evolution of the interior temperature for walls simulated with climate data from each city.

For walls simulated with climate data from the hot zone, the maximum temperatures for Wall type I, not exposed to rain and cloudiness, varied between 28.5 °C and 31 °C, and between 26.5 °C and 28.8 °C in case of exposure (Fig. 3a to Fig. 3d). The minimum temperature varied between 22 °C and 27 °C, and between 19 °C and 25 °C in the presence of rain and cloudiness. The cob wall with 6 % fibres (Type III) showed stable interior temperatures for all cities in the hot zone, except for Abidjan, where the temperature decreased from April to September. Regarding interior thermal comfort, clay walls do not provide the best thermal comfort in summer. When cloudiness and precipitation are considered, the temperatures of the interior surface always remain above 25 °C for the eight cities. However, the cob wall with 3 % fibres shows temperatures slightly above 27 °C for most of the summer

months, and the temperature of the interior surface of the cob wall with 6 % fibres is close to the comfort temperature set at 24 °C in summer throughout the year.

The maximum temperature for the wall type I, not exposed to rain and cloudiness, varied between 28 °C and 30 °C, while in the presence of these elements, it varied between 24 °C and 25 °C, for cities in the cold zone (from Fig. 3e to Fig. 3h). The minimum temperature was 17 °C for the four cities, and in case of exposure to rain and cloudiness, it was between 13 °C and 15 °C. There is no heating in the modeling, which mean that additional heating would be required. Temperatures above 25 °C were observed from the beginning of May to the end of September for clay walls. The cob wall with 3 % fibres (Type II) also recorded interior temperatures above 25 °C between May and September, except for the city of Reno. The cob wall with 6 % fibres (Type II) had stable interior temperatures with a maximum of 25 °C for all cities in the cold zone.

Considering the rate of cloudiness and precipitation leads to lower

temperatures of the surface of the interior walls compared to a simulation where these parameters are not considered. This demonstrates the importance of the inclusion of these parameters to accurately predict the thermal behaviour of construction materials. Nonetheless, whether the cob wall contains 6 % fibres or not, and whether it is exposed to heavy rain or not, it remains an acceptable option for the construction of bioclimatic buildings.

The humidity profile at a depth of 12.5 cm in the walls (marked by the blue dot), when subjected to the climates of each city, with or without exposure to driving rain and cloudiness, is presented in Fig. 4. As the exterior climate varies over time in both simulation cases (WUFI Pro 6.7 and COMSOL 6.1), humidity fluctuations are more pronounced for walls that are either exposed or not exposed to hourly cloudiness and precipitation, at a depth of 12.5 cm from the walls. Relative humidity greater than 80 % is observed at this depth in clay and cob walls with 3 % fibres, exposed to driving rain throughout the year for the cities of Abidjan, Montreal, Paris, and Rennes (Fig. 4d, 4e, 4f, and 4 g). For the cob wall with 6 % fibres, a fluctuation of relative humidity throughout

the wall was observed, and it always remains above 80 % throughout the year. For walls simulated with the climate data of Djibouti, Johannesburg, and Cairo, the humidity at 12.5 cm depth remains below 80 % throughout the year (Fig. 4a, 4b, and 4c), except for the city of Reno where the humidity fluctuates but remains below 80 % for most days of the year (Fig. 4 h). According to Künzel et al. [87], the risk of mold formation significantly increases when relative humidity exceeds 80 % for more than two weeks. Excluding driving rain and cloudiness from the simulations, the humidity profile at 12.5 cm depth is below 70 %. Fig. 5 illustrates the evolution of humidity through the walls, simulated with the climate data of Montreal and Rennes. Between 5 cm and 20 cm in depth, the humidity varies between 60 % and 50 % and remains constant between 10 cm and 15 cm for the clay wall. For cob walls, between 5 cm and 20 cm in depth, the humidity maintains between 70 % and 50 % and remains constant between 10 cm and 15 cm in depth in both cities. On the exterior surface of the walls, at 0 cm, a humidity of around 90 % is observed, thus a risk of water vapour condensation.

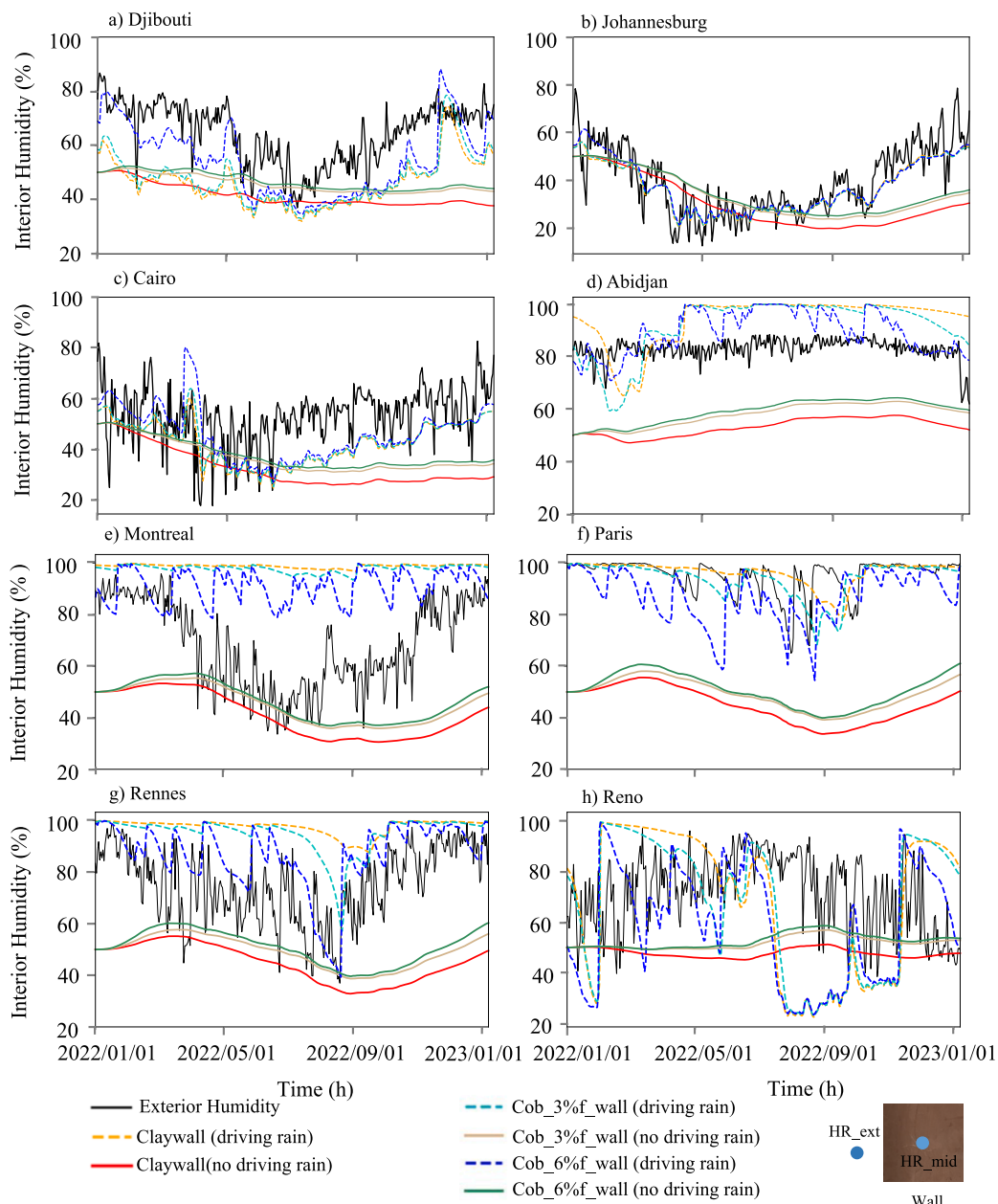


Fig. 4. Influence of driving rain on the humidity at 12.5 cm of uncoated clay and cob walls for the eight cities studied.

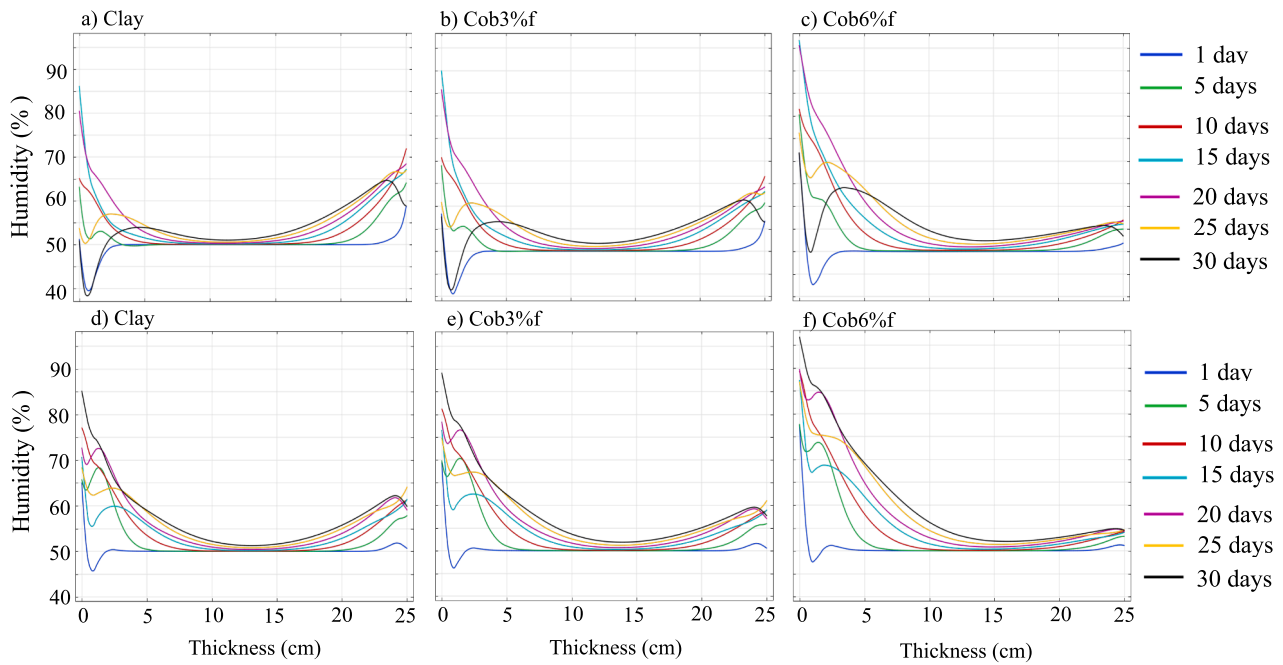


Fig. 5. Evolution of humidity through the walls: a to c) Montreal and d to f) Rennes cities.

3.2. Evaluation of humidity of the wall Type IV to Type IX

After observing the influence of driving rain and cloudiness rates on the moisture profile at a depth of 12.5 cm of clay and cob walls under different climatic conditions (Figs. 4 and 5), the evaluation subsequently focused on multilayer cob walls. The average moisture for two

consecutive months, from February 1st to April 1st (two-month average), was evaluated in order to identify the risk of mold in these walls (Fig. 6). Six multilayer walls were simulated with the climatic data of each city, and the configuration of these wall systems is presented in Tables 1 and 2, section 2.2. The simulation results indicated that the multilayer configurations type IV and V showed daily and two-month

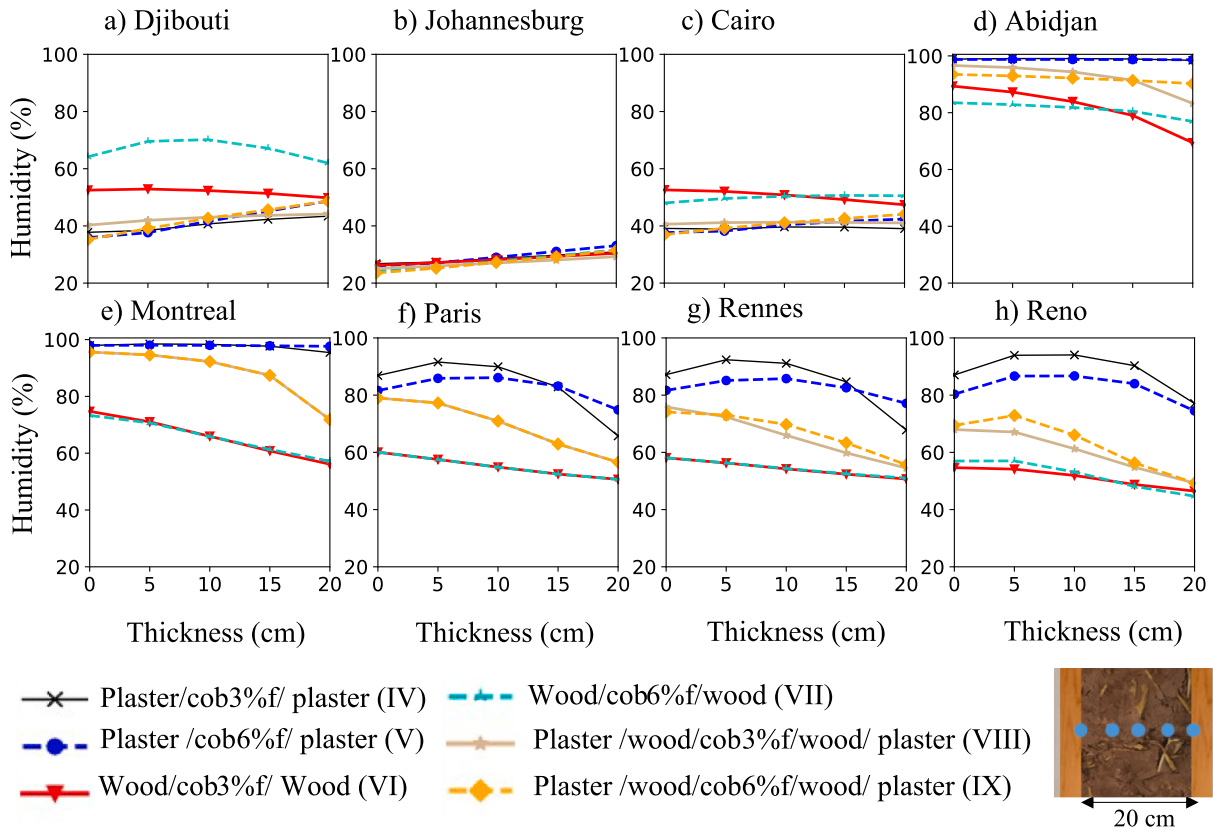


Fig. 6. Average humidity over two months (February, March) at each blue point indicated on the wall (for all walls, humidity is assessed at the same positions), for the eight cities studied. (For interpretation of the references to colour in this figure legend, the reader is referred to the web version of this article.)

average humidity levels above 80 % for the Paris, Rennes, and Reno cities. Moreover, in addition to configurations IV and V, the multilayer configurations VIII and IX also showed humidity rates above 80 % throughout the thickness of the cob walls for Montreal City. All walls displayed humidity rates above 80 % throughout the thickness of the cob walls when simulated with the climatic data of Abidjan city. This issue of lack of drying of the wall components for the Abidjan city can be mainly attributed to the high cloudiness rate of 0.71 with a maximum rain amount of about 25 L/m²/h and a very high precipitation duration compared to the other cities (Figure S8 in the supplementary document). In contrast, the humidity variation in all configurations remains below 70 % for the Djibouti, Johannesburg, and Cairo cities.

3.3. Interior heat and humidity flow

Fig. 7 illustrates the heat flow profile on the inner surface of cob walls, while Fig. 8 shows the seasonal average of this flow. A positive flow indicates a heat gain, which shows that heat moves from the wall surface to the interior environment, while a negative flow indicates a heat loss, with heat moving from the interior to the wall surface. In hot zones, Djibouti displayed a positive thermal flow throughout the year (Fig. 7a and 8a). The interior surfaces of walls, simulated with climate data of the Johannesburg and Cairo cities, showed a loss of heat flow in winter and autumn, and a gain in summer (Fig. 7b to 7c and 8b to 8c). In Abidjan, a decrease of thermal flow is observed in summer for type IV and V walls, and a gain in winter and autumn (Fig. 7d and 8d). This decrease can be attributed to driving rain, temperature drops, and the lack of clear sky to allow the walls to dry normally after a rainstorm. This leads to a loss of heat from the walls to allow them to dry or balance the interior environment's temperature.

The results reveal predominantly negative thermal flow throughout the year, except for a few days in summer, in cities of cold zones (Fig. 7e to 7h and 8e to 8h). Type IV and V walls recorded a heat loss varying between 0 and 70 W/m². Heat losses increase when the temperature drops and humidity rises. However, examining the simulation results, a

wall with a timber-frame structure allows for a reduction in heat losses, leading to a decrease in energy consumption for heating. The use of cob materials for the structure of timber-frame buildings significantly reduced the heat losses from the interior surface of the walls. Moreover, heat flow is stable with the amount of fibres present in the cob.

In terms of seasonal average, the wall type IV, made of a plaster/cob containing 3 % fibres/plaster, showed the most significant thermal losses, with values of about 40 W/m² in Montreal, 23.8 W/m² in Paris, 25 W/m² in Rennes, and 16 W/m² in Reno (Fig. 8e to 8g). Type VII wall showed low thermal losses for all cities in the cold zone. The addition of a clay plaster led to an increase in heat losses. For cities in the hot zone, Johannesburg and Cairo recorded thermal losses of about 10 W/m² and 6 W/m² in winter, while in Abidjan, the loss was about 13 W/m² for the wall of type V (plaster/cob with 6 % fibres/plaster). Conversely, in Djibouti, a positive thermal flow was observed throughout the year for all simulated walls.

As for heat flow, a positive moisture flow indicates a transfer of moisture from the the wall surface to the interior of the building, thereby increasing the humidity of the interior environment. Conversely, a negative moisture flow corresponds to a loss of moisture, with moisture moving from the interior to the wall surface. A significant increase in moisture flow in the walls can harm their durability and the building's thermal comfort. This can damage the wall materials, promote mold growth, reduce energy efficiency, and compromise the occupants' well-being. Fig. 9 illustrates the moisture flow profile on the interior surface of cob walls, while Fig. 10 shows the seasonal average of this flow.

For walls of type IV and V simulated with data from cold zone cities and the city of Abidjan, moisture flow showed considerable variability. For the rest of the cities in the hot zone, the maximum moisture flow for walls of types VI and VII was relatively low. The different local climatic conditions influence the water behaviour of the walls and the management of moisture. On a seasonal average, the moisture flow of type IV and V walls varied significantly for all simulations conducted with data from each city. The moisture flows are positive for all types of walls examined, with a tendency of moisture flow approaching zero for walls

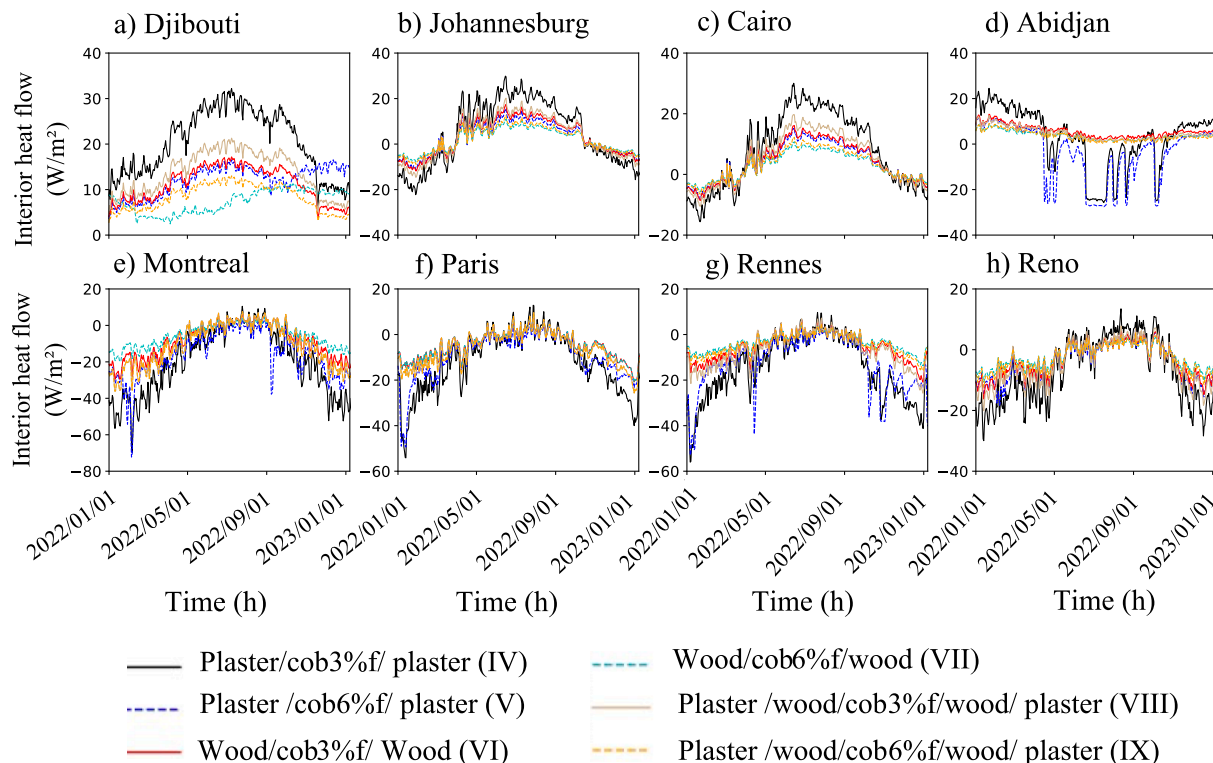


Fig. 7. Heat flow profile of the interior wall surfaces for the eight cities studied.

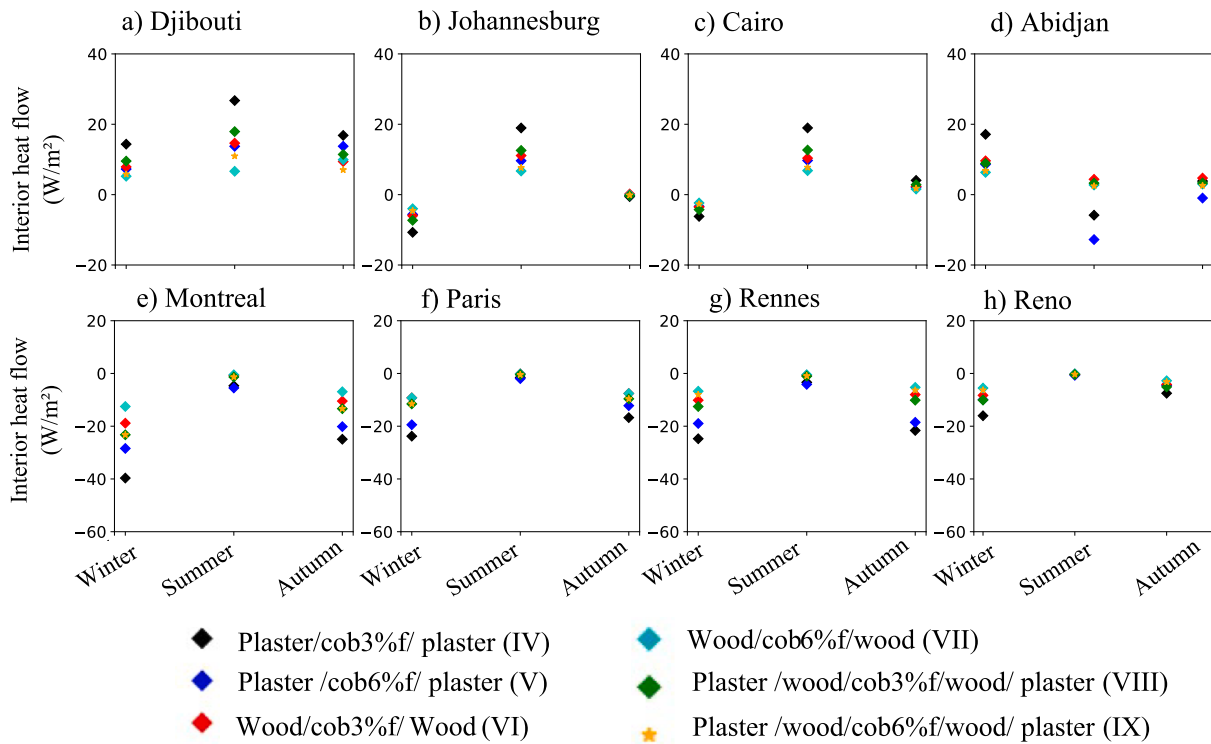


Fig. 8. Seasonal average heat flow of the interior wall surfaces for the eight cities studied.

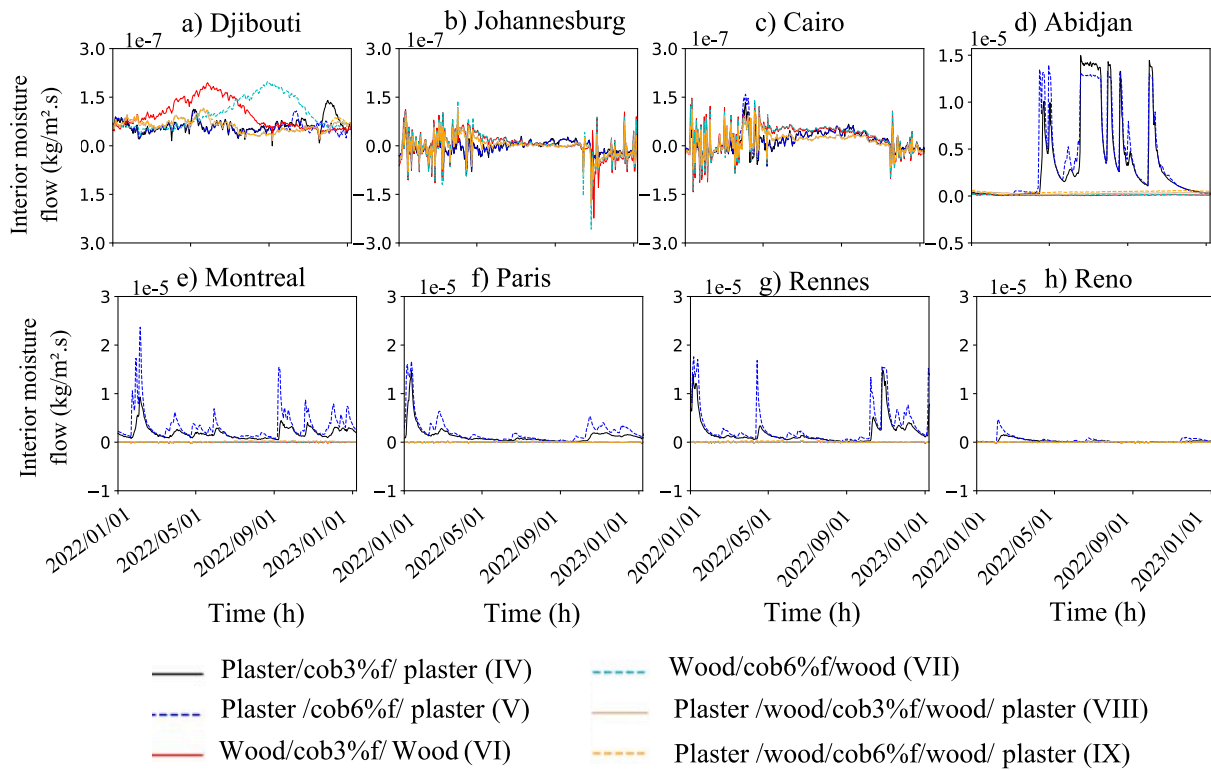


Fig. 9. Moisture flow profile of the interior wall surfaces for the eight cities studied.

of type VI to IX. It is crucial to note that incorporating fibres into the cob significantly increases the moisture absorption capacity, thus playing a vital role in regulating interior humidity and, by extension, in the comfort and health of the occupants.

4. Discussion

The humidity values, as well as the heat and moisture flow in the walls, are critical parameters for assessing hygrothermal behaviour. These are influenced by varying climatic conditions and the properties

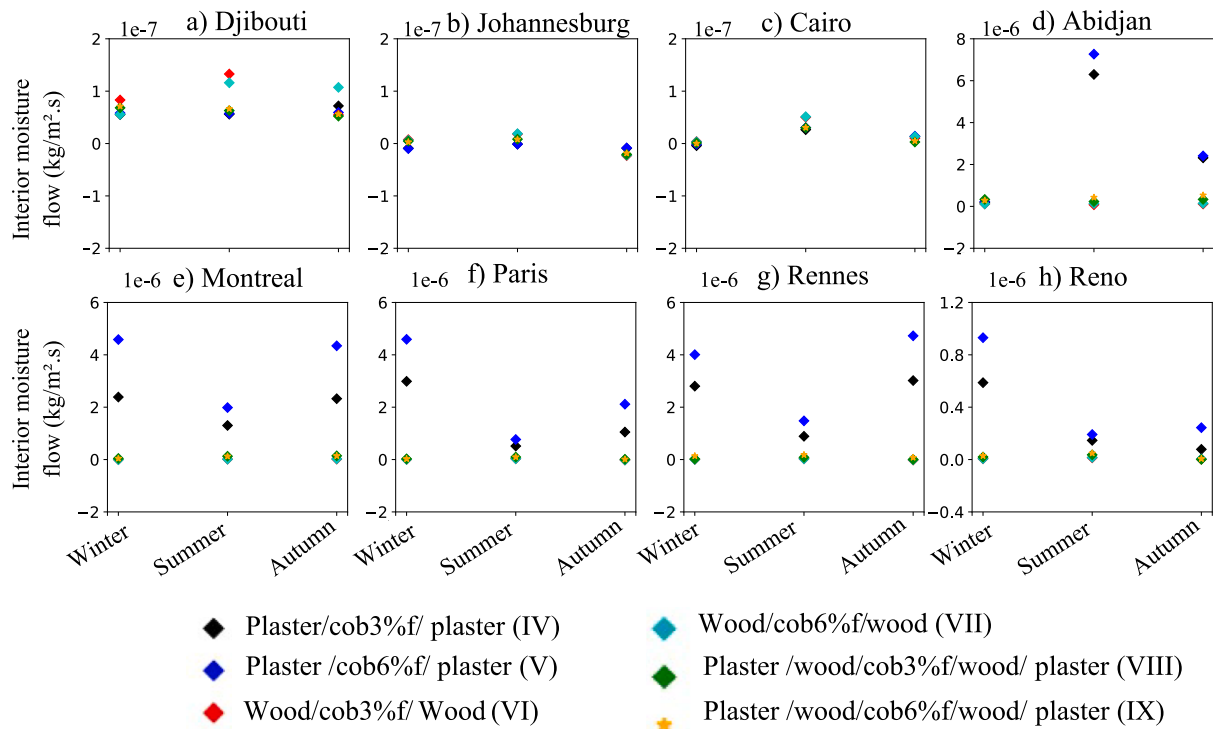


Fig. 10. Seasonal average moisture flow of the interior wall surfaces for the eight cities studied.

of the materials used, such as clay, cob, and other wall components. To assess the hygrothermal performance of these materials against different external climates, hygrothermal simulations were conducted using COMSOL 6.1 and WUFI Pro 6.7 for nine walls, including eight cob walls and one clay wall. Of the eight cob walls, six are multilayered and two are single-layered. The single-layer clay wall serves as a reference for the two single-layer cob walls. These simulations provided insights into

temperature, humidity variations, and heat and moisture flow over time, based on the climatic data specific to each city used for the simulation. The climatic data, encompassing both cold and warm climate countries, offer an idea of the hygrothermal performance of cob materials in different climatic zones. For instance, various authors have found good consistency between the results of numerical simulations and on-site measured data for walls constructed with earth materials [88,89],

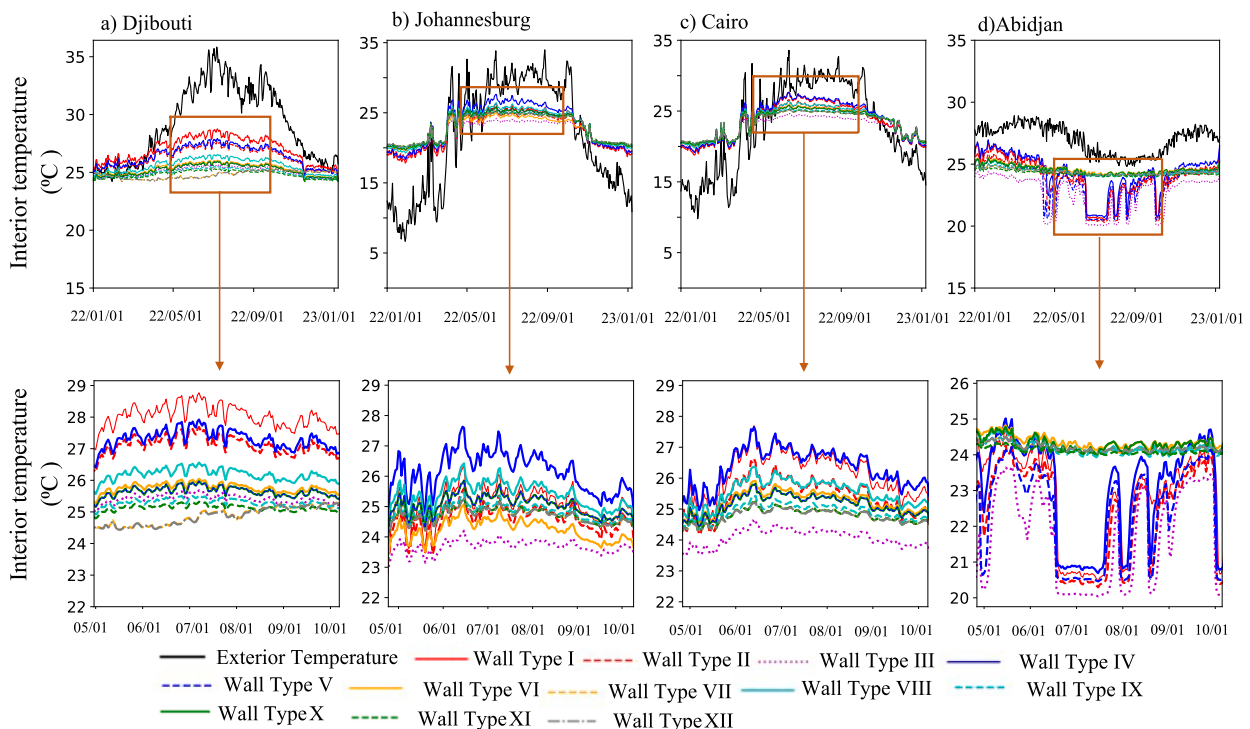


Fig. 11. Daily interior wall surface temperature in hot period.

geosourced materials [90], and biosourced materials [22,23,91–93].

4.1. Thermal performance of the walls

In terms of thermal performance, earth construction materials are recognized for their ability to regulate temperature and humidity [94–96]. According to all simulations conducted with COMSOL 6.1 and WUFI Pro 6.7, compiling climatic data, the temperature of the interior surface of clay walls varied between 12 °C (in the coldest city) and 29.6 °C (in the hottest city), this is for exterior temperatures from –15 °C to 43 °C (see Figs. 3, 11, and 12).

Multi-layer walls, simulated with the climatic data of the hot zone and with little cloud cover (see Table 3 and Fig. 11a, 11b, and 11c), showed temperatures of the interior surface of the walls varying between 24 °C and 26 °C for Djibouti and between 19.5 °C and 21 °C for Johannesburg and Cairo in winter. During summer and autumn, these temperatures varied from 24.3 °C to 26.6 °C for Djibouti, and from 21 °C to 26 °C for Johannesburg and Cairo.

Regarding cob walls, although types II to V, VIII, and IX are not suitable for very cold climates or those with significant precipitation and dense cloud cover, their ability to regulate interior temperature remains satisfactory (see Fig. 11d and 12). The use of a wooden structure or a vapour/air barrier for the design of cob buildings would improve thermal performance, with an increase in the minimum temperature of the interior surface of single-layer walls from 14 °C to 17 °C, an increase of 3 °C. Moreover, multi-layer walls made of cob with 6 % fibres (types V, VII, IX to XII) offer better interior comfort, with interior temperatures varying from 17 °C to 20 °C in winter, 20 °C to 25 °C in summer, and 21 °C to 15 °C in autumn, facing average daily exterior temperatures oscillating between –15 °C and 35 °C. Walls types VI, VII, XI, and XII, combining wood and cob, showed average daily interior temperatures varying from 18 °C to 25 °C. It is recommended to keep the temperature of the interior surface of the walls in cold areas above 12.6 °C [40], and this criterion has been met by the cob walls with a minimum

temperature of 14 °C.

The design of cob walls proves advantageous in hot climates, as it helps reduce the need for air conditioning. However, in cold climates, using cob requires special attention, particularly because of the serious problems that wall drying during construction can pose. These problems are related to humidity and very low temperatures, which lead to delays in the drying of the walls and cause an accumulation of moisture in the walls. For a construction made of earth or cob, it is necessary to prioritize multi-layer walls by adding additional layers to the wall and, beforehand, to use prefabricated and dry earth or cob materials to reduce drying time on the construction site. Construction should also be planned for warmer and drier seasons to avoid risks related to humidity and freezing.

4.2. Evaluation of mold growth in the walls

To assess the risk of mold development in different types of simulated walls, the WUFI Pro 6.7 software uses the LIM (Lowest Isoleth for Mould) model [97]. A moisture isopleth for building materials is a line drawn on a diagram connecting points of constant moisture throughout a material. This graphical representation allows visualization of how moisture distributes within the material under different environmental conditions. Analyzing moisture isopleths is essential for understanding the hygroscopic behavior of materials, assessing risks of mold, or degradation, and optimizing the thermal and sustainable performance of constructions. In practice, this helps engineers and architects design more resilient structures and prevent moisture-related issues. This model defines two categories of substrates, taking into account relative humidity, temperature, and the effect of construction materials. The LIM I category pertains to biodegradable materials used in construction, such as wallpaper and materials for permanent elasticity joints. The LIM II category, on the other hand, applies to porous construction materials. The analysis of the materials of the simulated walls in this study is based on the LIM II curve. Events below the LIM II curve indicate no risk of

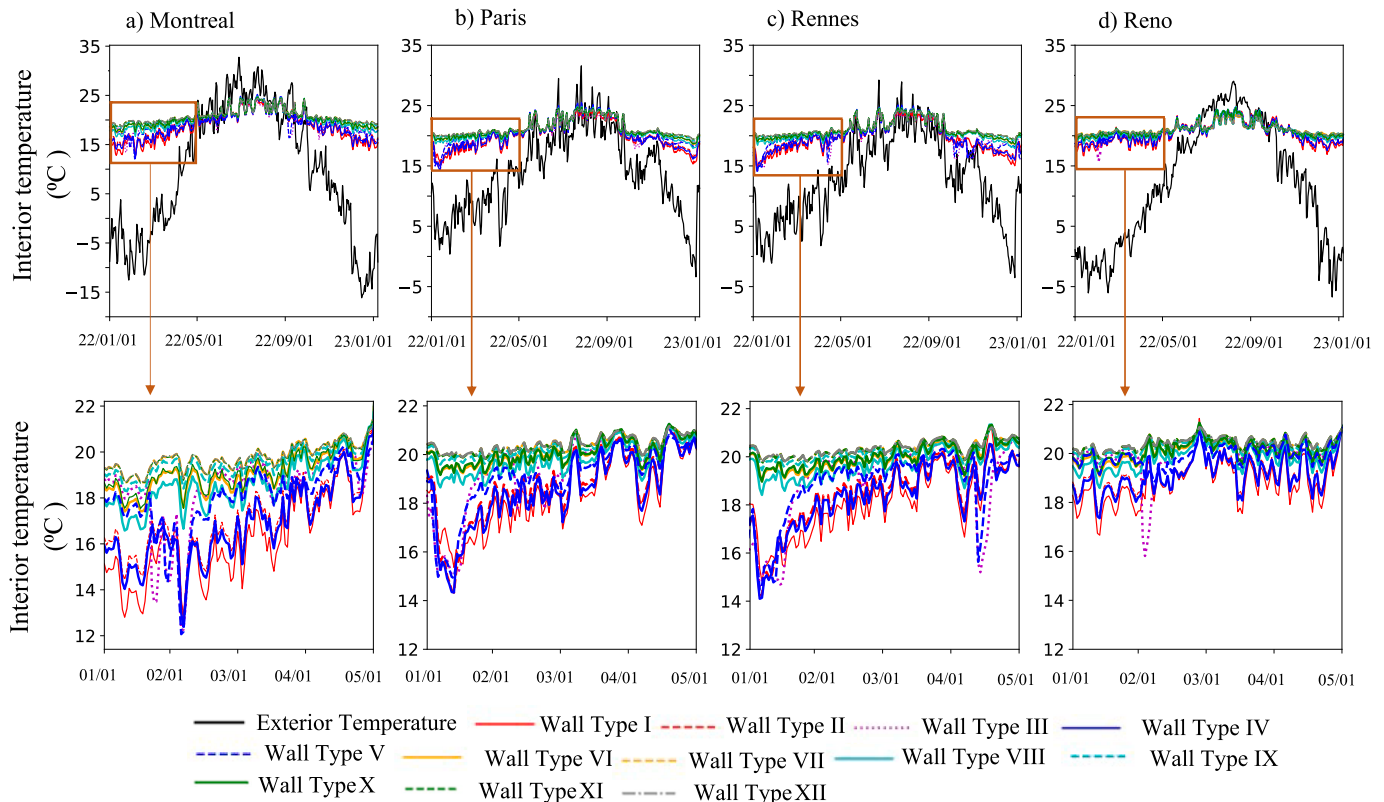


Fig. 12. Daily interior wall surface temperature in cold period.

mold in the walls, while events above this curve signal a risk of mold development. Data from an experimental study obtained for rock wool walls of buildings were compared with the results provided by WUFI Pro to evaluate the risk of mold in the insulation [97]. The simulation results and those obtained in situ were in agreement. Thus, the mold risk analyses presented in this section can be used realistically.

When analyzing the results of the simulated walls with various climate data, a significant impact of the finishing layers on the hygrothermal performance of the walls was also observed, as reported by other authors [98,99]. When the layer of clay plaster is applied to both sides of the walls, the greater the wall's moisture absorption. Given the severity of the climate, using materials such as clay or cob for construction especially in cold climate zones might not be suitable if the walls do not have adequate protection against driving rain, rainwater runoff, and capillary rise. The evolution of average humidity over two months through the walls, illustrated by Fig. 6, shows that the wood/cob/wood wall systems (Type VI and VII) is adapted to the climates of Montreal, Paris, Rennes, and Reno (Table S1 and S2 in the supplementary document). However, applying clay plaster to the exterior and interior sides of these walls (Type VIII and IX) presented a risk of water vapour condensation within the cob material, potentially leading to the rotting of fibres due to a humidity level exceeding 80 % throughout the material's thickness for the city of Montreal. Therefore, wall systems configured with cob material with 6 % fibres and air/vapor barriers for northern regions (Type X to Type XII walls), have been evaluated for high-risk cities observed in this study, Montreal and Abidjan cities.

All wall systems were suited to the climates of Djibouti, Johannesburg, and Cairo, with humidity levels below 80 % throughout the thickness of the cob throughout the year, except for the results obtained with the climate data of Abidjan (Fig. 4d and 6d). The humid tropical climate of Abidjan, characterized by a high cloudiness rate and a

maximum driving rain of 25 l/(m².h), increases the moisture absorption in the walls. For the walls to be adapted to such a climate, the foundations must be designed with a low water absorption coefficient to limit capillary rise and be covered by a steeply pitched roof to reduce rain-water runoff on the wall surfaces. To thoroughly evaluate the risk of mold growth in cob walls, key parameters (isopleths) considering relative humidity and temperature, generated by WUFI Pro, as well as climates presenting a high risk to cob walls, such as those of Abidjan and Montreal (evolution of humidity in the walls presented by Fig. 6d and 6e), were used.

The isopleths for walls of types IV, V, VIII, and IX showed that the hygrothermal conditions in the city of Montreal were conducive to mold growth, with numerous events located above the LIM II curve (Fig. 13a, 13b, 13e, and 13f). A low concentration of temperature/relative humidity events above the LIM II curve is observed for the exterior surface of the cob in contact with wood for walls of types VI and VII (Fig. 13c and 13d), indicating a low risk of mold development for these two types of walls. For wood and cob walls, when a clay plaster is applied to both exterior and interior sides, a high risk of mold is observed on the exterior surface and in the middle of the two walls, while the risk is low for the interior surface of the wall of type IX. A high concentration of temperature/relative humidity events above the LIM II curve was noted for all walls simulated with the climate data of Abidjan (Fig. 14). Tables S1 and S2 presented in the supplementary document summarize the hygrothermal conditions for 3 years of all walls simulated with different climate data. It is important to note that the results used for the mold growth risk analysis considering scenarios of heavy driving rain, representing the worst case of wall orientation.

According to Ghadie et al. [63], the use of a material that delays the transmission of water vapour placed just on the exterior side of the cob material could be an effective strategy to avoid the risk of mold

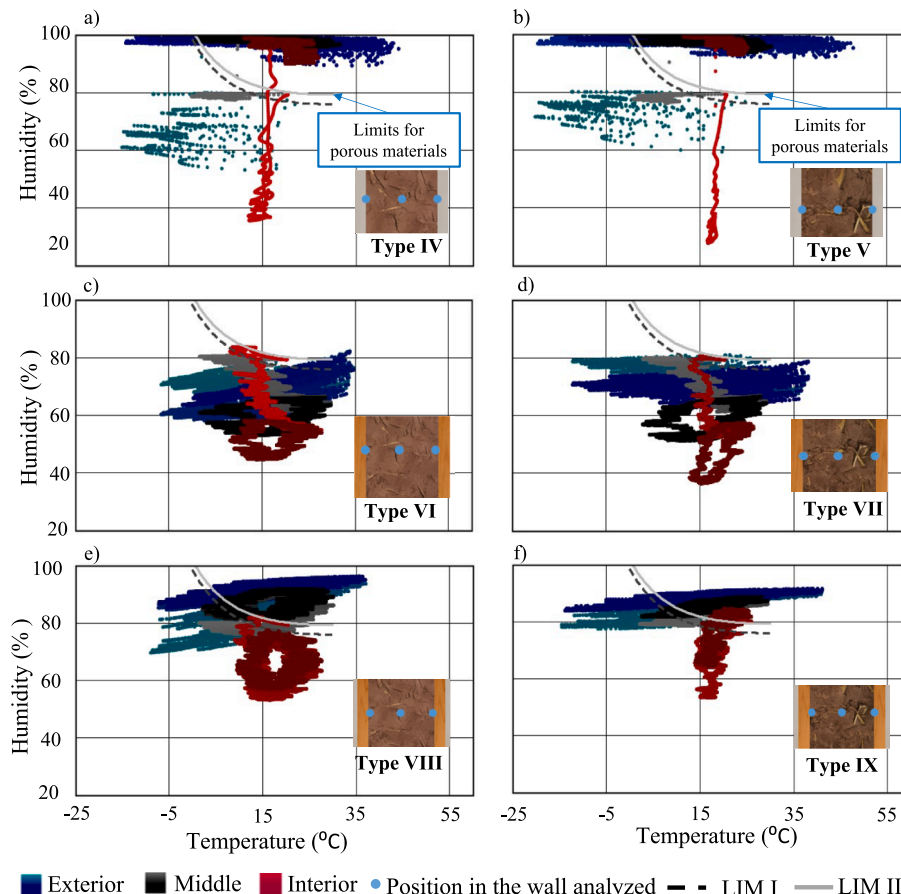


Fig. 13. Walls isopleths, exterior, middle, and interior sides of cob simulated with Montreal climate data.

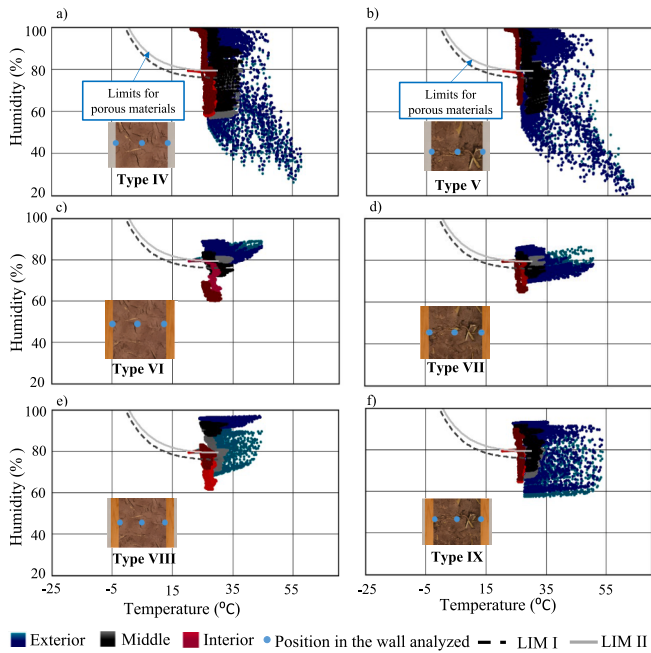


Fig. 14. Walls isopleths, exterior, middle, and interior sides of cob simulated with Abidjan climate data.

development. They also observed that adding a rain screen on the exterior of the wall could reduce the infiltration of rainwater and humidity, thereby protecting the wall materials against the accumulation of water vapour [63]. Consequently, wall systems with air/vapour barrier were modeled using the climate data of Abidjan and Montreal, two cities with high cloudiness rates. The air/vapour barrier was placed on the exterior side of the cob material. The isopleths generated for the

exterior surface, the middle, and the interior surface of the cob indicate a significant reduction in the risk of mold development, even in the worst-case scenario of wall orientation (Fig. 15). There is almost no concentration of temperature/relative humidity events above the LIM II curve for these walls simulated with the climate data of Abidjan and Montreal. This is visible when comparing Fig. 13a and Fig. 14a versus Fig. 15a to 15f. This means that there is no risk of mold development in the cob material, indicating that this type of design is suitable for cold climates and heavy rainfall.

5. Conclusion

Eco-friendly building design strategies, including traditional approaches, can significantly reduce the environmental impact of buildings while maintaining thermal comfort. This study explored the use of materials such as clay and cob for constructing single and multilayer walls to analyze their hygrothermal performance, heat and moisture losses or gains, and the risk of mold development. The conclusions drawn from the simulation results are as follows:

- By analyzing the evaluation of humidity variation across the walls, based on simulation data covering the period from February 1 to March 31, and the assessments of the risk of mold appearance for wall configurations IV to XII over three years of simulation, we find that the higher the cloudiness index, the more the walls tend to accumulate moisture, which increases the risk of mold development.
- All wall configurations demonstrated good hydric performance in the cities of Djibouti, Johannesburg, and Cairo. For the cities of Montreal, Paris, Rennes, and Reno, the configurations using exclusively wood as a structure show superior hydric performance compared to other configurations. In contrast, for the city of Abidjan, the configurations that meet the humidity performance standards correspond to wall types X to XII.

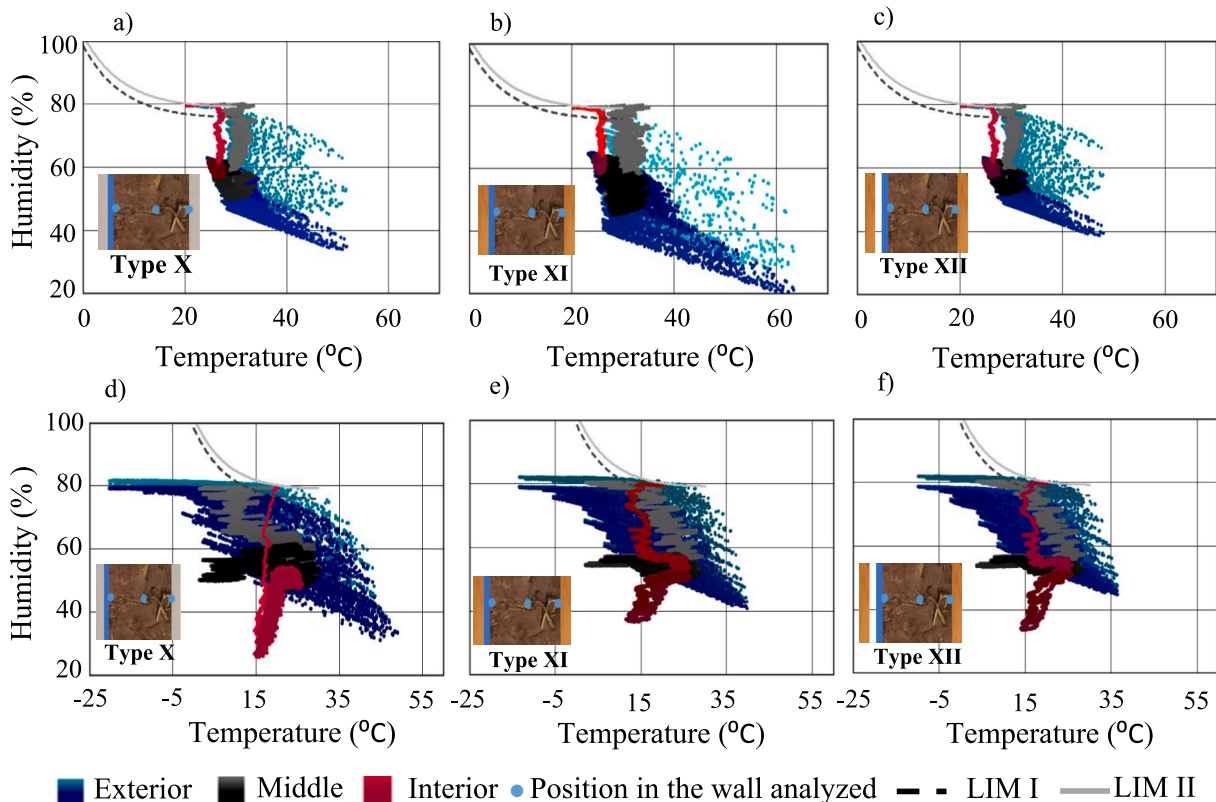


Fig. 15. Isopleth for the Type X to XII walls with air/vapour barrier on the cob: a, b, c) Abidjan and d, e, f) Montreal.

- Single-layer cob walls, especially those containing 6 % fibres, provide more favourable interior temperatures for both cold and hot climate zones. For exterior temperatures varying from $-15\text{ }^{\circ}\text{C}$ to $43\text{ }^{\circ}\text{C}$, the variation in interior surface temperatures was $12\text{ }^{\circ}\text{C}$ to $29.6\text{ }^{\circ}\text{C}$ for clay walls, $15\text{ }^{\circ}\text{C}$ to $27\text{ }^{\circ}\text{C}$ for cob walls with 3 % fibres, and $19\text{ }^{\circ}\text{C}$ to $25.5\text{ }^{\circ}\text{C}$ for cob walls with 6 % fibres. Considering cloud cover and driving rain results in a significant reduction in the maximum interior temperature of the simulated walls. Moreover, applying a clay finish and using a wooden structure for cob walls enhance interior thermal comfort, thus reducing the heating demand to maintain interior temperatures above $21.9\text{ }^{\circ}\text{C}$ in winter, and the cooling demand for interior temperatures below $26\text{ }^{\circ}\text{C}$ in summer. The temperatures of cob walls with 6 % fibres are more stable, regardless of the boundary conditions used for the simulation.
- Regarding moisture management in walls, clay plaster significantly impacts the hygrothermal behaviour of simulated cob walls. Applying finishes, whether on a cob or wooden structure, causes a significant increase in wall moisture. This increase can lead to a heightened risk of mold formation, especially in walls exposed to cold climate conditions or heavy rainfall. Walls simulated with the climatic data of cities in the cold and damp zones were particularly vulnerable, except for types VI, VII, and Types X to XII, which did not present a risk of mold.
- The use of an air/vapour barrier or rain screen on the exterior side of the cob material eliminates the risk of mold development.
- For hot and low precipitation climatic zones, the use of clay finishes proves to be beneficial for good temperature and humidity regulation.

In conclusion, cob materials are a viable alternative for current construction and can be used as an infill material for wood-frame structures, provided that the wall design is adapted to specific climatic zones. Cob walls not only reduce interior thermal discomfort but also heat and moisture losses through the walls. The results presented in this article are the results of the evaluation of the hygrothermal performance of standard walls, which are promising.

Based on the results presented in this article, further studies are necessary to complete this research:

- Conduct numerical modeling at the building scale: Perform numerical modeling of entire cob buildings to evaluate their hygrothermal performance.
- Carry out experimental measurements at the building scale: Implement experimental measurements over a period of one year or more to confirm the hygrothermal benefits of wood/cob structures.
- Evaluate the impact of roofs: Analyze the hygrothermal behavior of cob buildings with roofs of different slopes by conducting in situ measurements to observe the influence of heavy rain on cob walls associated with a wooden structure.
- Given that the WUFI Pro 6.7 and COMSOL 6.1 models have been validated with data from other types of materials, it would be necessary to validate both models with experimental data from cob walls, whether with 3 % or 6 % fibres.
- Evaluate the comfort parameters in the numerical model to account for specific regions, population groups, and/or modeling approaches.

CRedit authorship contribution statement

Aguerata Kabore: Writing – original draft, Visualization, Software, Methodology, Investigation, Formal analysis, Data curation, Conceptualization. **Mathieu Bendouma:** Writing – review & editing, Software, Conceptualization. **Claudiane Ouellet-Plamondon:** Writing – review & editing, Validation, Supervision, Resources, Project administration, Methodology, Investigation, Funding acquisition, Data curation, Conceptualization.

Declaration of competing interest

The authors declare that they have no known competing financial interests or personal relationships that could have appeared to influence the work reported in this paper.

Acknowledgments

The author wants to thank the Pole de Recherche et d'Innovation en Matériaux avancés du Québec (PRIMA Québec (PRIMAR20-13-008)), the Natural Sciences and Engineering Research Council of Canada (NSERC) Alliance program (CRSNG ALLRP 560404-2020), Mitacs (IT35572), Québec Wood Export Bureau (QWEB), American Structures, Technologies Boralife inc., ENERGIES 2050, and the Canada Research Chair on Sustainable Multifunctional Construction Materials (CRC-2019-00074) to support this study.

Appendix A. Supplementary data

Supplementary data to this article can be found online at <https://doi.org/10.1016/j.enbuild.2025.115351>.

Data availability

Data will be made available on request.

References

- [1] A. Alioui, S.I. Kaitouni, Y. Azalam, E.M. Bendada, M. Mabrouki, *Effect of straw fibers addition on hygrothermal and mechanical properties of carbon-free adobe bricks: From material to building scale in a semi-arid climate*, Build. Environ. 255 (2024) 111380, <https://doi.org/10.1016/j.buildenv.2024.111380>.
- [2] S. Bouckaert, A. F. Pales, C. McGlade, U. Remme, B. Wanner, L. Varro, D. D'Ambrosio and T. Spencer, *Net zero by 2050: A roadmap for the global energy sector*. (2021) <https://iea.blob.core.windows.net/assets/063ae08a-7114-4b58-a34e-39db2112d0a2/NetZeroBy2050-ARoadmapfortheGlobalEnergySector.pdf>.
- [3] X. Hu, L. Xie, Z. Chen, P. Lei, H. Chen, T. Tan, *Study on the uniaxial compression constitutive relationship of modified yellow mud from minority dwelling in western Sichuan, China*. Reviews on Advanced Materials Science 62 (1) (2023) 20220291, <https://doi.org/10.1515/rams-2022-0291>.
- [4] P. Walker, B.V. Reddy, M. Mani, *Preface for SI: Modern earth building materials and technologies*, Constr. Build. Mater. 262 (2020) 120663, <https://doi.org/10.1016/j.conbuildmat.2020.120663>.
- [5] L. Xie, X. Hu, Z. Xu, Z. Chen, P. Wang, R. Liang, *Experimental study on comprehensive improvement of shear strength and erosion resistance of yellow mud in Qiang Village*, Rev. Adv. Mater. Sci. 61 (1) (2022) 795–816, <https://doi.org/10.1515/rams-2022-0040>.
- [6] P. Muñoz, V. Letelier, L. Muñoz, D. Zamora, *Assessment of technological performance of extruded earth block by adding bottom biomass ashes*, J. Build. Eng. 39 (2021) 102278, <https://doi.org/10.1016/j.job.2019.101122>.
- [7] D.L. Samuel, K. Dharmasastha, S.S. Nagendra, M.P. Maiya, *Thermal comfort in traditional buildings composed of local and modern construction materials*, Int. J. Sustain. Built Environ. 6 (2) (2017) 463–475, <https://doi.org/10.1016/j.ijsbe.2017.08.001>.
- [8] Y.E. Belarbi, M.Y. Ferroukhi, N. Issaadi, P. Poullain, S. Bonnet, *Assessment of hygrothermal performance of raw earth envelope at overall building scale*, Energ. Buildings (2024) 114119, <https://doi.org/10.1016/j.enbuild.2024.114119>.
- [9] F. Alassaad, K. Touati, D. Levacher, N. Sebaibi, *Effect of latent heat storage on thermal comfort and energy consumption in lightweight earth-based housings*, Build. Environ. 229 (2023) 109915, <https://doi.org/10.1016/j.buildenv.2022.109915>.
- [10] T. De Mets, A. Tilmans, X. Loncour, *Hygrothermal assessment of internal insulation systems of brick walls through numerical simulation and full-scale laboratory testing*, Energy Procedia 132 (2017) 753–758, <https://doi.org/10.1016/j.egypro.2017.10.022>.
- [11] G. Giuffrida, L. Ibos, A. Boudenne, H. Allam, *Exploring the integration of bio-based thermal insulations in compressed earth blocks walls*, Constr. Build. Mater. 418 (2024) 135412, <https://doi.org/10.1016/j.conbuildmat.2024.135412>.
- [12] K. Haddad, S. Lannon, E. Latif, *Investigation of Cob construction: Review of mix designs, structural characteristics, and hygrothermal behaviour*, J. Build. Eng. (2024) 108959, <https://doi.org/10.1016/j.job.2024.108959>.
- [13] F. Dejeant, P. Garnier, and T. Joffroy, *Matériaux locaux, matériaux d'avenir*. (2021) CRAterre. <https://hal.science/hal-03293589>.
- [14] C. Hema, A. Messan, A. Lawane, D. Soro, P. Nshimiyanima, G. Van Moeseke, *Improving the thermal comfort in hot region through the design of walls made of compressed earth blocks: An experimental investigation*, J. Build. Eng. 38 (2021) 102148, <https://doi.org/10.1016/j.job.2021.102148>.

- [15] M. Gomaa, S. Schade, D.W. Bao, Y.M. Xie, Automation in rammed earth construction for industry 4.0: Precedent work, current progress and future prospect, *J. Cleaner Production* 398 (2023), <https://doi.org/10.1016/j.jclepro.2023.136569>.
- [16] M. Gomaa, J. Vaculik, V. Soebarto, M. Griffith, W. Jabi, *Feasibility of 3DP cob walls under compression loads in low-rise construction*, *Constr. Build. Mater.* 301 (2021) 124079, <https://doi.org/10.1016/j.conbuildmat.2021.124079>.
- [17] M. Schweiker, E. Endres, J. Gossler, N. Hack, L. Hildebrand, M. Creutz, A. Klinge, H. Kloft, U. Knaack, J. Mehnert, *Ten questions concerning the potential of digital production and new technologies for contemporary earthen constructions*, *Build. Environ.* 206 (2021) 108240, <https://doi.org/10.1016/j.buildenv.2021.108240>.
- [18] D. El-Mahdy, H.S. Gabr, S. Abdelmohsen, *SaltBlock as a 3D printed sustainable construction material in hot arid climates*, *J. Build. Eng.* 43 (2021) 103134, <https://doi.org/10.1016/j.job.2021.103134>.
- [19] M.M. Bühler, P. Hollenbach, A. Michalski, S. Meyer, E. Birle, R. Off, C. Lang, W. Schmidt, R. Cudmani, O. Fritz, *The Industrialisation of Sustainable Construction: A Transdisciplinary Approach to the Large-Scale Introduction of Compacted Mineral Mixtures (CMMs) into Building Construction*, *Sustainability* 15 (13) (2023) 10677, <https://doi.org/10.3390/su151310677>.
- [20] A. Belabid, H. Elminor, H. Akhrouz, *Hybrid construction technology, towards a mix that satisfies the requirements of the 21st century: state of the art and future prospects*, *Future Cities Environ.* 8 (1) (2022), <https://doi.org/10.5334/fce.159>.
- [21] A. Kaboré, W. Maref, C.M. Ouellet-Plamondon, *Hygrothermal Performance of the Hemp Concrete Building Envelope*, *Energies* 17 (7) (2024) 1740, <https://doi.org/10.3390/en17071740>.
- [22] B. Moujalled, Y.A. Oumeziane, S. Moissette, M. Bart, C. Lanos, D. Samri, *Experimental and numerical evaluation of the hygrothermal performance of a hemp lime concrete building: A long term case study*, *Build. Environ.* 136 (2018) 11–27, <https://doi.org/10.1016/j.buildenv.2018.03.025>.
- [23] N. Boumediene, F. Collet, S. Prétot, S. Elaoud, *Hygrothermal Behavior of a Washing Fines-Hemp Wall under French and Tunisian Summer Climates: Experimental and Numerical Approach*, *Materials* 15 (3) (2022) 1103, <https://doi.org/10.3390/ma15031103>.
- [24] M. Asli, F. Brachelet, E. Sassine, E. Antczak, *Thermal and hygroscopic study of hemp concrete in real ambient conditions*, *J. Build. Eng.* 44 (2021) 102612, <https://doi.org/10.1016/j.job.2021.102612>.
- [25] Y. Xu, Z. Zeng, *Experimental and numerical investigation on the effect of heat and moisture coupling migration of unsaturated lateritic clay for the soil thermal storage system*, *Energ. Buildings* 276 (2022) 112499, <https://doi.org/10.1016/j.enbuild.2022.112499>.
- [26] M. Bart, S. Moissette, Y. Ait Oumeziane, C. Lanos, *Transient hygrothermal modelling of coated hemp-concrete walls*, *Eur. J. Environ. Civil Eng.* 18 (8) (2014) 927–944, <https://doi.org/10.1080/19648189.2014.911122>.
- [27] D. Lelievre, T. Colinart, P. Glouannec, *Hygrothermal behavior of bio-based building materials including hysteresis effects: Experimental and numerical analyses*, *Energ. Buildings* 84 (2014) 617–627, <https://doi.org/10.1016/j.enbuild.2014.09.013>.
- [28] M. Benkhaled, S.-E. Ouldboukhitine, A. Bakkour, S. Amziane, *Sensitivity analysis of the parameters for assessing a hygrothermal transfer model HAM in bio-based hemp concrete material*, *Int. Commun. Heat Mass Transfer* 132 (2022) 105884, <https://doi.org/10.1016/j.icheatmasstransfer.2022.105884>.
- [29] F. Bennai, M.Y. Ferroukhi, F. Benmahiddine, R. Belarbi, A. Nouviaire, *Assessment of hygrothermal performance of hemp concrete compared to conventional building materials at overall building scale*, *Constr. Build. Mater.* 316 (2022) 126007, <https://doi.org/10.1016/j.conbuildmat.2021.126007>.
- [30] T. Colinart, D. Lelievre, P. Glouannec, *Experimental and numerical analysis of the transient hygrothermal behavior of multilayered hemp concrete wall*, *Energ. Buildings* 112 (2016) 1–11, <https://doi.org/10.1016/j.enbuild.2015.11.027>.
- [31] N. Reuge, F. Collet, S. Prétot, S. Moissette, M. Bart, O. Style, A. Shea, C. Lanos, *Hygrothermal effects and moisture kinetics in a bio-based multi-layered wall: Experimental and numerical studies*, *Constr. Build. Mater.* 240 (2020) 117928, <https://doi.org/10.1016/j.conbuildmat.2019.117928>.
- [32] D. Wu, M. Rahim, M. El Ganaoui, R. Bennacer, R. Djedjig, B. Liu, *Dynamic hygrothermal behavior and energy performance analysis of a novel multilayer building envelope based on PCM and hemp concrete*, *Constr. Build. Mater.* 341 (2022) 127739, <https://doi.org/10.1016/j.conbuildmat.2022.127739>.
- [33] Q. Gao, T. Wu, L. Liu, Y. Yao, B. Jiang, *Prediction of wall and indoor hygrothermal properties of rammed earth folk house in Northwest Sichuan*, *Energies* 15 (5) (2022) 1936, <https://doi.org/10.3390/en15051936>.
- [34] V. Toufigh, S. Samadianfard, *Experimental and numerical investigation of thermal enhancement methods on rammed-earth materials*, *Sol. Energy* 244 (2022) 474–483.
- [35] N. Laaroussi, et al., *Measurement of thermal properties of brick materials based on clay mixtures*, *Constr. Build. Mater.* 70 (2014) 351–361, <https://doi.org/10.1016/j.solener.2022.08.049>.
- [36] B. Jiang, T. Wu, W. Xia, J. Liang, *Hygrothermal performance of rammed earth wall in Tibetan Autonomous Prefecture in Sichuan Province of China*, *Build. Environ.* 181 (2020) 107128, <https://doi.org/10.1016/j.buildenv.2020.107128>.
- [37] L. Zhang, G. Sang, W. Han, *Effect of hygrothermal behaviour of earth brick on indoor environment in a desert climate*, *Sustain. Cities Soc.* 55 (2020) 102070, <https://doi.org/10.1016/j.scs.2020.102070>.
- [38] L. Laou, L. Ulmet, S. Yotte, J.-E. Aubert, P. Maillard, *Simulation of the Hygro-Thermo-Mechanical Behavior of Earth Brick Walls in Their Environment*, *Buildings* 13 (12) (2023) 3061, <https://doi.org/10.3390/buildings13123061>.
- [39] M. Charai, A. Mezרחab, L. Moga, *A structural wall incorporating bioinspired earth for summer thermal comfort improvement: Hygrothermal characterization and building simulation using calibrated PMV-PPD model*, *Build. Environ.* 212 (2022) 108842, <https://doi.org/10.1016/j.buildenv.2022.108842>.
- [40] M.R. Ahmad, B. Chen, Y. Maierdan, S.M.S. Kazmi, M.J. Munir, *Study of a new capillary active bio-insulation material by hygrothermal simulation of multilayer wall*, *Energy Build.* 234 (2021), <https://doi.org/10.1016/j.enbuild.2021.110724>.
- [41] A. Mellaikhaifi, M. Ouakarrouch, A. Benallel, A. Tilioua, M. Ettakni, A. Babaoui, M. Garoum, M.A.A. Hamdi, *Characterization and thermal performance assessment of earthen adobes and walls additive with different date palm fibers*, *Case Studies Constr. Mater.* 15 (2021), <https://doi.org/10.1016/j.cscm.2021.e00693>.
- [42] W. Schmidt, M. Commeh, K. Olonade, G.L. Schiewer, D. Dodoo-Arhin, R. Dauda, S. Fataei, A.T. Tawiah, F. Mohamed, M. Thiedeitz, *Sustainable circular value chains: From rural waste to feasible urban construction materials solutions*, *Dev. Built Environ.* 6 (2021) 100047, <https://doi.org/10.1016/j.dibe.2021.100047>.
- [43] L.F. Cabeza, C. Barreneche, L. Miro, J.M. Morera, E. Bartolí, A. Fernández, *Low carbon and low embodied energy materials in buildings: A review*, *Renew. Sustain. Energy Rev.* 23 (2013) 536–542, <https://doi.org/10.1016/j.rser.2013.03.017>.
- [44] B.V. Reddy, P.P. Kumar, *Embodied energy in cement stabilised rammed earth walls*, *Energ. Buildings* 42 (3) (2010) 380–385, <https://doi.org/10.1016/j.enbuild.2009.10.005>.
- [45] J. Fernandes, M. Peixoto, R. Mateus, H. Gervásio, *Life cycle analysis of environmental impacts of earthen materials in the Portuguese context: Rammed earth and compressed earth blocks*, *J. Clean. Prod.* 241 (2019) 118286, <https://doi.org/10.1016/j.jclepro.2019.118286>.
- [46] P. Mendonca, C. Vieira, *Embodied carbon and economic cost analysis of a contemporary house design using local and reused materials*, *Sustainable Futures* 4 (2022) 100100, <https://doi.org/10.1016/j.sfr.2022.100100>.
- [47] L.F. Cabeza, L. Boquera, M. Châfer, D. Vérez, *Embodied energy and embodied carbon of structural building materials: Worldwide progress and barriers through literature map analysis*, *Energ. Buildings* 231 (2021) 110612, <https://doi.org/10.1016/j.enbuild.2020.110612>.
- [48] L.A. Saba, M.H. Ahmad, R.A. Majid, A. Yahaya, *Material and assembly selection: Comparative analysis of embodied energy and carbon as an index for environmental performance*, *Journal of Advanced Research in Materials Science* 44 (1) (2018) 1–24.
- [49] E. Hamard, B. Cazacliu, A. Razakamanantsoa, J.C. Morel, *Cob, a vernacular earth construction process in the context of modern sustainable building*, *Build. Environ.* 106 (2016) 103–119, <https://doi.org/10.1016/j.buildenv.2016.06.009>.
- [50] C. Ouellet-Plamondon, A. Kabore, in: *Hygrothermal Measurement of Heavy Cob Materials*, Springer, 2023, https://doi.org/10.1007/978-3-031-33211-1_111.
- [51] Y. Taourite, A.-L. Tiffonnet, M. Marion, H. Louahli, M. El Alami, A. Gounni, E. Lépinasse, I. Voicu, *Effect of Temperature on Moisture Migration in Earth and Fiber Mixtures for Cob Materials*, *Energies* 16 (14) (2023) 5526, <https://doi.org/10.3390/en16145526>.
- [52] Y. Kang, H.H. Jo, S. Yang, S. Wi, S. Kim, *Numerical evaluation of indoor hygrothermal behavior with heat and moisture transfer in walls by analytical conditions*, *Appl. Thermal Eng.* 216 (2022), <https://doi.org/10.1016/j.applthermaleng.2022.11915>.
- [53] A. Fang, Y. Chen, L. Wu, *Modeling and numerical investigation for hygrothermal behavior of porous building envelope subjected to the wind driven rain*, *Energ. Buildings* 231 (2021) 110572, <https://doi.org/10.1016/j.enbuild.2020.110572>.
- [54] M. Wei, B. Wang, S. Liu, in: *Numerical Simulation of Heat and Moisture Transfer of Wall with Insulation*, IOP Publishing, 2019, <https://doi.org/10.1088/1742-6596/1300/1/012029>.
- [55] M. Tonini de Araújo, H.A. de Souza, A.P. Gomes, *Computer simulation of moisture transfer in walls: impacts on the thermal performance of buildings*, *Architect. Eng. Design Manage.* 18 (4) (2022) 453–472, <https://doi.org/10.1080/17452007.2021.1916426>.
- [56] A. Kabore, A. Laghdar, C. Ouellet-Plamondon, *Natural thermal and hygrothermal regulation with heavy cob for low carbon construction*, *Constr. Build. Mater.* 451 (2024) 138832, <https://doi.org/10.1016/j.conbuildmat.2024.138832>.
- [57] S. Yu, Y. Cui, Y. Shao, F. Han, *Simulation research on the effect of coupled heat and moisture transfer on the energy consumption and indoor environment of public buildings*, *Energies* 12 (1) (2019) 141, <https://doi.org/10.3390/en12010141>.
- [58] R. Belloum, B. Agoudjil, N. Chennouf, A. Boudenne, *Hygrothermal performance assessment of a bio-based building made with date palm concrete walls*, *Building Environ.* 223 (2022), <https://doi.org/10.1016/j.buildenv.2022.109467>.
- [59] H. Zhang, C. Shi, D. Pan, Y. Xuan, X. He, *Optimization of effective moisture penetration depth model considering airflow velocity for gypsum-based materials*, *J. Build. Eng.* 32 (2020), <https://doi.org/10.1016/j.job.2020.101539>.
- [60] J. Goffart, M. Rabouille, N. Mendes, *Uncertainty and sensitivity analysis applied to hygrothermal simulation of a brick building in a hot and humid climate*, *J. Build. Perform. Simul.* 10 (1) (2017) 37–57, <https://doi.org/10.1080/19401493.2015.1112430>.
- [61] V. Gerlich, K. Sulovská, M. Zálesák, *COMSOL Multiphysics validation as simulation software for heat transfer calculation in buildings: Building simulation software validation*, *Measurement* 46 (6) (2013) 2003–2012, <https://doi.org/10.1016/j.measurement.2013.02.020>.
- [62] Y. Chbani Idrissi, R. Belarbi, R. Allam, M.B. Feddaoui, F. Bennai, D. Agliz, *Experimental and numerical validation of hygrothermal transfer in brick wall*, *Heat Transfer* 50 (6) (2021) 6300–6327, <https://doi.org/10.1002/htj.22173>.
- [63] G. Tlajji, F. Pennec, S. Ouldboukhitine, M. Ibrahim, P. Biwolé, *Hygrothermal performance of multilayer straw walls in different climates*, *Constr. Build. Mater.* 326 (2022), <https://doi.org/10.1016/j.conbuildmat.2022.126873>.
- [64] J.H. Park, Y.U. Kim, J. Jeon, B.Y. Yun, Y. Kang, S. Kim, *Analysis of biochar-mortar composite as a humidity control material to improve the building energy and*

- hygrothermal performance, *Sci. Total Environ.* 775 (2021), <https://doi.org/10.1016/j.scitotenv.2021.145552>.
- [65] O. Douzane, G. Promis, J.M. Roucoult, A.D.T. Le, T. Langlet, *Hygrothermal performance of a straw bale building: In situ and laboratory investigations*, *J. Build. Eng.* 8 (2016) 91–98, <https://doi.org/10.1016/j.jobbe.2016.10.002>.
- [66] A. Mesa, A. Arenghi, *Hygrothermal behaviour of straw bale walls: experimental tests and numerical analyses*, *Sustainable Build.* 4 (2019). <https://hdl.handle.net/11379/524968>.
- [67] U. Dhakal, U. Berardi, M. Gorgolewski, R. Richman, *Hygrothermal performance of hempcrete for Ontario (Canada) buildings*, *J. Clean. Prod.* 142 (2017) 3655–3664, <https://doi.org/10.1016/j.jclepro.2016.10.102>.
- [68] M. Lamalle, Bloc de béton de bois, une alternative au bloc traditionnel? Étude des caractéristiques mécaniques, thermiques et écologiques d'un bloc de coffrage en béton de bois, U.d.L.L. Faculté des Sciences Appliquées, Belgium, Editor. 172 (2016). <http://hdl.handle.net/2268.2/1283>.
- [69] P. Brisebois, M. Aouinti, M. Jafari, M. Siaj C. Ouellet-Plamondon, *Adsorption Dynamics of Disodium Octaborate Tetrahydrate on Clay Minerals: Implications for Construction Wood Protection*. (2024) doi: 10.1002/smt.202400753.
- [70] A. Kabore, C.M. Ouellet-Plamondon, *Improved insulation with fibres in heavy cob for building walls*, *Ind. Crop. Prod.* 215 (2024) 118626, <https://doi.org/10.1016/j.indcrop.2024.118626>.
- [71] A. Kabore, C.M. Ouellet-Plamondon, *The Impact of Vegetable Fibres on the Shrinkage and Mechanical Properties of Cob Materials*, *Materials* 17 (3) (2024) 736, <https://doi.org/10.3390/ma17030736>.
- [72] H.M. Künzel, and F.I. Germany. Modeling Air Leakage in Hygrothermal Envelope Simulation. in Building Enclosure Science & Technology (BEST3) Conference, Atlanta, USA. 2012.
- [73] H.M. Künzel, *Simultaneous heat and moisture transport in building components*. One- and two-dimensional calculation using simple parameters, IRB-Verlag Stuttgart 65 (1995). <https://wufi.de/de/wp-content/uploads/sites/9/2014/12/K%3%BCnzel-1995-Simultaneous-Heat-and-Moisture-Transport1.pdf>.
- [74] D. Lelièvre, Simulation numérique des transferts de chaleur et d'humidité dans une paroi multicouche de bâtiment en matériaux biosourcés. (2015) Lorient. <https://theses.hal.science/tel-01250778>.
- [75] M. Bendouma, *Systèmes d'isolation thermique par l'extérieur: études expérimentales et numériques des transferts de chaleur et d'humidité*, Université de Bretagne Sud, 2018.
- [76] S. Kittiworawatt, S. Devahastin, *Improvement of a mathematical model for low-pressure superheated steam drying of a biomaterial*, *Chem. Eng. Sci.* 64 (11) (2009) 2644–2650, <https://doi.org/10.1016/j.ces.2009.02.036>.
- [77] R. Yang, A. Jia, S. He, Q. Hu, M. Sun, T. Dong, Y. Hou, S. Zhou, *Experimental investigation of water vapor adsorption isotherm on gas-producing Longmaxi shale: Mathematical modeling and implication for water distribution in shale reservoirs*, *Chem. Eng. J.* 406 (2021) 125982, <https://doi.org/10.1016/j.cej.2020.125982>.
- [78] Y.H. Roos, *Water sorption modeling and monolayer of biological and food materials*, *LWT* (2024) 116271, <https://doi.org/10.1016/j.lwt.2024.116271>.
- [79] L. Evangelisti, C. Guattari, F. Asdrubali, *On the sky temperature models and their influence on buildings energy performance: A critical review*, *Energ. Buildings* 183 (2019) 607–625, <https://doi.org/10.1016/j.enbuild.2018.11.037>.
- [80] M. Ibrahim, L. Bianco, O. Ibrahim, E. Wurtz, *Low-emissivity coating coupled with aerogel-based plaster for walls' internal surface application in buildings: energy saving potential based on thermal comfort assessment*, *J. Build. Eng.* 18 (2018) 454–466, <https://doi.org/10.1016/j.jobbe.2018.04.008>.
- [81] ANSI/ASHRAE 55, *ASHRAE Standard 55: Thermal environmental conditions for human occupancy*. (2004), American Society of Heating, Refrigerating and Air-Conditioning Engineers. [http://www.ditar.cl/archivos/Normas ASHRAE/T0080ASHRAE-55-2004-ThermalEnviroCondiHO.pdf](http://www.ditar.cl/archivos/Normas%20ASHRAE/T0080ASHRAE-55-2004-ThermalEnviroCondiHO.pdf).
- [82] F. Collet, L. Serres, J. Miriel, M. Bart, *Study of thermal behaviour of clay wall facing south*, *Build. Environ.* 41 (3) (2006) 307–315, <https://doi.org/10.1016/j.buildenv.2005.01.024>.
- [83] P.M. Toure, Y. Dieye, P.M. Gueye, M. Faye, V. Sambou, *Influence of envelope thickness and solar absorptivity of a test cell on time lag and decrement factor*, *J. Build. Phys.* 43 (4) (2020) 338–350, <https://doi.org/10.1177/1744259119863446>.
- [84] A.P. Nelson, *Etude De Matériaux Biosourcés Pour L'isolation Thermique Des Bâtiments En Climat Tropical Humide*, Antilles (2020). <https://theses.fr/2020ANT10517>.
- [85] T. Colinart, M. Bendouma, and P. Glouannec, *Simulation du comportement hygrothermique d'une façade opaque ventilée de bâtiment*. in *Congrès SFT*. (2019). <https://www.researchgate.net/publication/334202332>.
- [86] Weather API, *Historical weather data collection*. 2012–2024. <https://openweathermap.org/api>.
- [87] H. Künzel, A. Holm, D. Zirkelbach, A. Karagiozis, *Simulation of indoor temperature and humidity conditions including hygrothermal interactions with the building envelope*, *Solar energy* 78 (4) (2005) 554–561, <https://doi.org/10.1016/j.solener.2004.03.002>.
- [88] A.A. Hamid, P. Wallentén, *Hygrothermal assessment of internally added thermal insulation on external brick walls in Swedish multifamily buildings*, *Build. Environ.* 123 (2017) 351–362, <https://doi.org/10.1016/j.buildenv.2017.05.019>.
- [89] M. Guizzardi, D. Derome, J. Carmeliet, *Water uptake in clay brick at different temperatures: experiments and numerical simulations*, *J. Build. Phys.* 39 (4) (2016) 373–389, <https://doi.org/10.1177/1744259115578227>.
- [90] A. Alioui, S.I. Kaitouni, Y. Azalam, E.M. Bendada, M. Mabrouki, *Effect of straw fibers addition on hygrothermal and mechanical properties of carbon-free adobe bricks: From material to building scale in a semi-arid climate*, *Build. Environ.* (2024), <https://doi.org/10.1016/j.buildenv.2024.111380>.
- [91] D. Bastien, M. Winther-Gaasvig, J. Zhang Andersson, Z. Xiao, H. Ge, *Hygrothermal performance of natural building materials: Simulations and field monitoring of a case study home made of wood fiber insulation and clay*, *J. Build. Phys.* 47 (3) (2023) 249–283, <https://doi.org/10.1177/17442591231195639>.
- [92] S. Dubois, A. Evrard, F. Lebeau, *Modeling the hygrothermal behavior of biobased construction materials*, *J. Build. Phys.* 38 (3) (2014) 191–213, <https://doi.org/10.1177/1744259113489810>.
- [93] M. Defo, M. Lacasse, A. Laouadi, *A comparison of hygrothermal simulation results derived from four simulation tools*, *J. Build. Phys.* 45 (4) (2022) 432–456, <https://doi.org/10.1177/1744259120988760>.
- [94] G. Giada, R. Caponetto, F. Nocera, *Hygrothermal properties of raw earth materials: A literature review*, *Sustainability* 11 (19) (2019) 5342, <https://doi.org/10.3390/su11195342>.
- [95] L.M. Lalicata, A.W. Bruno, and D. Gallipoli. *Hygro-thermal coupling in earth building materials*. in *E3S Web of Conferences*. (2023) EDP Sciences. doi: 10.1051/e3sconf/202338223003.
- [96] M. Wakil, H. El Mghari, S.I. Kaitouni, R. El Amraoui, *Thermal energy performance of compressed earth building in two different cities in Moroccan semi-arid climate*, *Energy Built Environ.* 5 (5) (2024) 800–816, <https://doi.org/10.1016/j.enbenv.2023.06.008>.
- [97] I. Apine, M. Birjukovs, A. Jakovics, *Comparative assessment of mould growth risk in lightweight insulating assemblies via analysis of hygrothermal data and in situ evaluation*, *J. Ecol. Eng.* 20 (11) (2019). <https://doi.org/10.12911/22998993/113147>.
- [98] J. Maia, N.M. Ramos, R. Veiga, *Evaluation of the hygrothermal properties of thermal rendering systems*, *Build. Environ.* 144 (2018) 437–449, <https://doi.org/10.1016/j.buildenv.2018.08.055>.
- [99] J. Maia, M. Pedroso, N. Ramos, P. Pereira, I. Flores-Colen, M.G. Gomes, L. Silva, *Hygrothermal performance of a new thermal aerogel-based render under distinct climatic conditions*, *Energy Build.* 243 (2021), <https://doi.org/10.1016/j.enbuild.2021.111001>.